

ALMA MATER STUDIORUM - UNIVERSITÀ DI BOLOGNA

SCHOOL OF ENGINEERING AND ARCHITECTURE

*DEPARTMENT OF CIVIL, CHEMICAL, ENVIRONMENTAL AND MATERIALS
ENGINEERING*

MASTER'S DEGREE IN OFFSHORE ENGINEERING

THESIS

in

*OFFSHORE HSE MANAGEMENT ****

WIND LOAD EFFECT ON STORAGE TANKS IN AZERBAIJAN

Candidate

TURAN MUTALLIMOV

Supervisor:

Prof. ERNESTO SALZANO

Co-supervisor

Academic Year [2020-2021]

Session IV

Summary

Nomenclature	3
1. Introduction	5
2. State of the art	7
2.1 Storage Tanks and Strong Winds	7
2.1.2 Strong winds hazard	7
2.1.2 Winds in Azerbaijan	8
2.1.3 Storage tanks classifications	12
2.1.4 Classification of oil storage tanks using in Azerbaijan	16
2.2 Accidents scenario	19
2.2.1 Natural hazards	20
2.2.2 Natech Risk	22
2.2.3 Storage tank accidents	23
2.2.4 Definition of potential accidental scenarios	28
2.2.5 Analyses of structural and natural hazards	31
3. Materials and methods	32
3.1 Storage tanks damage by strong winds	32
3.1.1 Shell buckling	32
3.1.2 Overturning	37
3.1.3 Impact of debris	38
3.2 Wind load effects (local standard TN and Q 2.01.07-85)	43
3.2.1 Structures parameters and Wind loads	43
3.2.2 Calculation of wind load	43
3.2.3 Peak wind load	47
3.2.4 Calculation of wind load effect on storage tanks	52
4. Results and discussions	54
4.1 Calculation results of wind effect (API 620 and API 650)	54
4.1.1 Shell buckling	54
4.1.2 Overturning	58
4.1.3 Impact of the object	60
4.2 Calculation results of wind effect (TN and Q 2.01.07-85)	63
4.2.1 Calculation of wind loading	64
4.3 Comparison of the results	70
5. Conclusions	73
6. Bibliography	75

Nomenclature

f	Frequency of natural hazards	K_d	Wind directionality factor
t_r	Inverse of the	I	Importance factor
h [m]	Design liquid level	G	Gust factor
D [m]	Nominal tank diameter	V	3 sec gust wind speed at 10 m for open terrain exposure
CA [m]	Corrosion allowance	C_p	Wind pressure coefficient
S_d [MPa]	Allowable stress for the design condition	θ	Longitude measured from windward
P_r	Resistance pressure	α_i	Fourier coefficient
P_f	Pressure from the stored fluid	q_{eq} [Pa]	Equivalent uniform external pressure
P_{cr}	Material resistance pressure of the tank	p_{max}	Maximum non-uniform pressure
E	Modulus of elasticity	C_θ	External buckling factor for medium-length cylinders
t	Shell thickness	ω	Relative length parameter for the shell
H	Height of the tank	F_p	Pressure combination factor
n	Parameter to minimize critical pressure	M_{pi}	Moment about the shell-to-bottom joint from design internal pressure
ν	Poisson coefficient.	M_w	Overturning moment about the shell-to-bottom joint from horizontal plus vertical wind pressure
K_z	Velocity pressure exposure coefficient	M_{DL}	Moment about the shell-to-bottom joint from the nominal weight of the shell and roof structural supported by

K_{zt}	Topographic factor	M_F	the shell that is not attached to roof plate Moment about the shell-to-bottom joint from the liquid weight
$\rho_w [kg/m^3]$	Wind density	M_{DLR}	Moment about the shell-to-bottom joint from the nominal weight of the roof plate plus any attached structural
$A_p [m^2]$	Object area	$U_0 [m/s]$	Impact speed
C_F	Aerodynamic force coefficient	$M [kg]$	Object mass
$\rho_p [kg/m^3]$	Density of the debris material	$\sigma_D [Pa]$	Dynamic yield stress
h_p	Penetration depth	$r_p [m]$	Object radius
$d_p [m]$	Object diameter	$f_u [Pa]$	ultimate strength
q	dynamic wind pressure	$\epsilon_u [Pa]$	ultimate strain of the targets constitutive material
V	basic wind speed	Ae	effective area
h	height of element	Def	effective diameter
t _{ins}	insulation thickness	Di	internal diameter
w ₀	wind pressures	β	inclination
v ₊₍₋₎	correlation coefficient		

1. Introduction

There is no industry that is immune to a significant accident caused by the unintentional release of energy and dangerous materials. Such accidents may be caused by operational failures, such as the accident in a Union Carbide chemical factory in Bhopal, India, where maintenance failures and operating procedures resulted in an aberrant leak of methylisocyanate that spread across the city, resulting serious health problems and sometimes even deaths to hundreds of individuals, as well as economic loss to the company (Eckerman, 2005). Accidents, on the other hand, may be caused by natural phenomena including such earthquakes, tsunamis, wind gusts, and other environmental catastrophes. Hurricane Floyd, for example, wreaked havoc on the petroleum industry on the eastern part of the United States and Canada, spilling thousands of tons of fuel, gasoline, and chemicals, resulting in massive environmental damage and immense financial damage (Young et al., 2004).

Natural disasters have become more common over the last few decades. Cruz et al. (2004) confirmed in 2004 that various extreme physical events have been on the rise over time. Between 1980 and 1989, the analysis was performed around the United States, yielding the below-mentioned information: 228 earthquakes, 26 hurricanes, 16 flooding, 15 thunderstorms, 13 blizzards, and 7 storms have struck the United States this year. Furthermore, 1022 floods occurred globally in the 1990s, while the frequency of these natural disasters has risen by 74% over the last decade (CRED, 2019).

Oil prices fluctuate significantly due to political and economic factors; currently, the United States, Japan, and other developing countries have formed a full petroleum reserve system; however, most countries have not yet finished the strategic reserve inventory, so it is critical to increase the strategic petroleum reserve base. These logistical issues will undoubtedly continue to evolve in the direction of large-scale and large-amount oil storage tanks, while oil storage tanks will be severely affected, and casualties will be higher in the event of an earthquake.

Oil storage tanks in hazardous areas are not only endangered by earthquakes, but they are also often affected by strong winds while in operation. Traditional non-isolation oil storage tanks frequently have insufficient seismic capability, making them vulnerable to destruction during an earthquake. Once the harm happens, it will result in significant economic losses; however, the leakage of special materials will result in secondary disasters such as waste material and fire; and the most important case is that people's lives will be negatively impacted.

In Azerbaijan, over the country, as evaluated, the great part of the petroleum industry is located in windy locations. During the year, mostly, the speed of wind can reach the 40 m/s and over. For construction of oil storage tanks local and global standards are using. In case of, windy weather condition above-mentioned natural hazards, the stability of the tanks are calculated, and the results compared between

different standards in the calculation part of the thesis. As a result, given the significant risk that natural hazards pose to industrial facilities, particularly equipment which warehouses large amounts of hazmat, this thesis scope focuses on the impact of strong winds on reservoirs built to API 620, API 650 and TN and Q 2.01.07-85 which is mainly used in Azerbaijan (based on СП 20.13330.2011 СНиП 2.01.07-85 Russian standard).

2. State of the art

2.1 Storage Tanks and Strong Winds

Many authors believe that storage tanks are the most vulnerable to severe winds such as tornadoes, hurricanes, and storms (Burgos et al., 2014). However, in order for such types of natural events to impact or harm a storage tank, it must be empty or partly full (0-10% fill level) (Uematsu et al., 2014; Zhao & Lin, 2014). As a result, the most important final outcome of the Natech incident would be the damage or failure of process equipment, rather than the loss of hazmat containment (Maraveas et al., 2015).

2.1.2 Strong winds hazard

It is really important to remember that wind is a random complex concept that changes over time and space (Simiu and Yeo, 2019). The wind speed is typically determined by its velocity and direction. From zero at ground level to an equilibrium position at a height that determines the boundary condition, wind speed increases with height. The level of the boundary layer can depend upon the type of terrain roughness, which is generally described as increasing roughness from open water to open terrain, suburban, and finally industrial exposes. The relationship between wind speed and height is usually logarithmic or power law. In addition, the magnitude of the velocity is determined by the reference time period on which the wind speed is averaged. 3 sec gusts, 1 minute wind gusts, and 10-minute wind gusts seem to be the most common time periods used to describe wind loads. For the same reason, the wind velocity decreases as the averaging time lengthens.

Since wind is a moving fluid, its effect is a mixture of aerostatic and aerodynamic pressure that are proportional to the square of the wind velocity. Different requirements around the world suggest different formulas for computing wind pressures (for example, ASCE 7-16 in the United States (American Society of Civil Engineers, 2017)), but in general, they all have wind maps for defined return periods t_r , where the engineer can choose a design wind speed based on the facility's position and significance. Different variables are then applied to the basic wind velocity pressure equations to account for issues such as topography, terrain visibility, altitude, and so on. The velocity pressures are therefore compounded by non-dimensional exterior pressure coefficients that are dependent on the structure's design and the wind's movement with reference to it. Internal pressure coefficient multiplies the velocity pressure to produce internal stresses, which are dependent on the structure's transparency. The final effect is a distribution of equal static design pressures common to the structure for low-rise, comparatively stiff structures like oil tanks.

Tropical cyclones, for example, are known for their strong winds (hurricanes in the Western Hemisphere; typhoons in the Eastern Pacific; cyclones in the Indian Ocean). These are most common over warm ocean waters at low latitudes and are particularly dangerous due to their disruptive ability. Hurricanes in the

Western Hemisphere are categorized using the Saffir/Simpson hurricane scale (see Table 1). Hurricanes have 1-minute sustained wind speeds at 10 m over open seas that are equal to or greater than 120 km/h, as seen in Table 1. (74 mph).

Table 1.

Extreme winds are classified according to their strength or vector of effects.
(Allaby, 2007; Potter & Colman, 2003)

Wind load	Hurricane category	Hazard classification	Wind speed (Km/h)	Storm surge (m)
Low load	1	Very low	119 – 153	1.2 – 1.5
Medium load	2	Low	154.4 – 177	1.8 – 2.4
High load	3	Moderate	178.5 – 209	2.7 – 3.6
	4		210 – 249	3.9 – 5.4
Very high load	5	High	>250	>5.4

Since tropical cyclones are spinning storms, the path of the winds that affect an industrial facility during a storm can vary based on the facility's position relative to the eye. The wind direction may change 180 degrees as the eye moves over the facility if this is in the direction of the eye.

2.1.2 Winds in Azerbaijan

The climate in Azerbaijan is generally continental, with relatively warm summers and cold winters; it is also barren in most low-lying regions, while the mountains are cooler and rainier. The Caspian Sea coast is semi-arid in the north and arid in the middle, while the southernmost stretch is rainy, constituting an exception to the law that Azerbaijan's plains are arid. Azerbaijan's winters are cold but not freezing, particularly in the plains. The Caucasus Mountain Range protects the country's interior from cold air outbreaks from Russia; in reality, the north wind descending from the mountains is warm and dry, similar to the Foehn or Chinook, while the cold wind flows strongly along the coastline but is balanced by the Caspian Sea. In the winter, however, there might be light snowfalls and frosts along the coast, but particularly inland, where cold air can easily stagnate after the wind has vanished.

Azerbaijan petroleum industry is mainly located in Baku and Caspian Sea where the strong winds are dominating. To clarify the real wind situation over the country, winds are classified as follows in globally, locally in Azerbaijan and in the Caspian region as well.



Figure 1. Location of Azerbaijan (Baku) in map

Table 2

Windstorm : Scales and Effects										
Beaufort Scale						Saffir–Simpson Hurricane Scale				
Bft	Descriptive term	Mean wind speed at 10 m above surface			Wind pressure Kg/m ²	SS	Descriptive term	Mean wind speed		
		m/s	Km/h	knots				m/s	Km/h	knots
0	Calm	0–0.2	0–1	0–1	0	1	Weak	32.7–42.6	118–153	64–82
1	Light air	0.3–1.5	1–5	1–3	0–0.1	2	Moderate	42.7–49.5	154–177	83–96
2	Light breeze	1.6–3.3	6–11	4–6	2.0–0.6	3	Strong	49.6–58.5	178–209	97–113
3	Gentle breeze	3.4–5.4	12–19	7–10	0.7–1.8	4	Very strong	58.6–69.4	210–249	114–134
4	Moderate breeze	5.5–7.9	20–28	11–15	1.9–3.9	5	Devastating	≥ 69.5	≥ 250	≥ 135
5	Fresh breeze	8.0–10.7	29–38	16–21	4.0–7.2	Fujita Tornado Scale				
6	Strong breeze	10.8–13.8	39–49	22–27	7.3–11.9	F	Descriptive term	m/s	Km/h	Knots
7	Near gale	13.9–17.1	50–61	28–33	12.0–18.3	0	Weak	17.2–32.6	62–117	34–63
8	Gale	17.2–20.7	62–74	34–40	18.4–26.8	1	Moderate	32.7–50.1	118–180	64–97
9	Strong gale	20.8–24.4	75–88	41–47	26.9–37.3	2	Strong	50.2–70.2	181–253	98–136
10	Storm	24.5–28.4	89–102	48–55	37.4–50.5	3	Devastating	70.3–92.1	254–332	137–179
11	Violent storm	28.5–32.6	103–117	56–63	50.6–66.5	4	Annihilating	92.2–116.2	333–418	180–226
12	Hurricane	> 32.7	> 118	> 64	> 66.6	5	Disaster	116.3–136.9	419–493	227–266

Baku is known as the City of Winds (Azerbaijani: Külöklər şəhri), owing to the fact that it is windy for the majority of the year. Baku is characterized by two winds: the cold and strong Khazri and the warm and gentle Gilavar. The cold north Caspian Sea wind known as Khazri (Azerbaijani: Xəzri) blows across the Absheron Peninsula all year, especially in Baku. Khazri is a gale-force coastal wind that is one of the area's dominant winds. Khazri can attain speeds of up to 40 m/s (140 km/h; 89 mph; 78 kn). It has a negative impact on certain economic sectors. During the summer, however, the wind keeps the temperature cool. The Khazri wind is the polar opposite of the Gilavar, a warm southerly breeze that can be felt in the season. Gilavar is the southern wind that blows throughout the year in eastern Azerbaijan, especially in Baku and Shamakhi. It is captured in the direction from the land to the sea and is mainly observed in the summer months. However, observation is possible in other seasons of the year. When the summer months, it increases the temperature of the air, reduces humidity, and the temperature in the winter and in the spring.

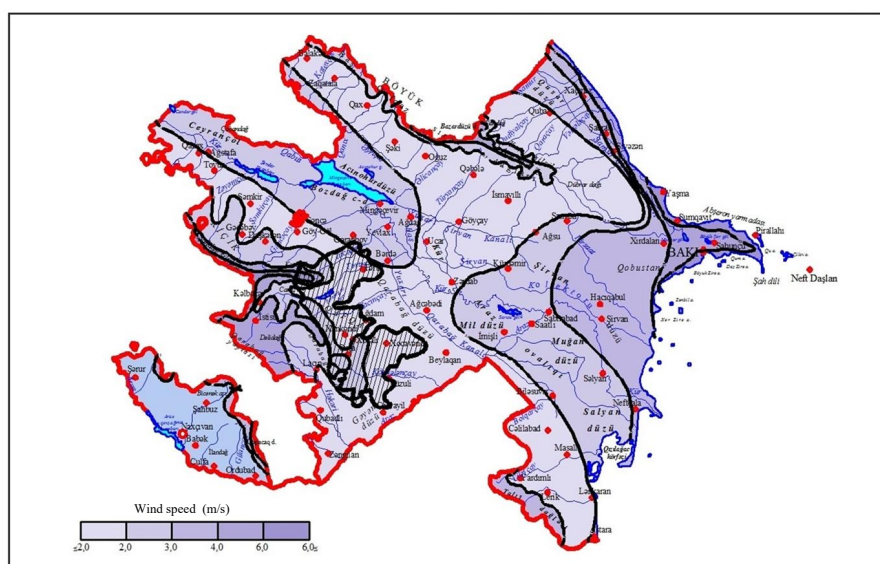


Figure 2. *Zoning of the territory of the Republic of Azerbaijan according to the average annual wind speed*

Because the Caspian stretches for a long distance in the meridional direction and is located in two climatic zones (subtropical and temperate), the meteorological conditions are different in different parts of it.

For the northern part of the Caspian Sea, east and south-east winds prevail in the annual course. North-west and south-east winds dominate the Middle Caspian. For the Absheron region, north and south winds prevail due to the influence of orography.

The main criterion for the zoning of the sea was the wind speed (15 m / s). The most frequent winds are observed in the Absheron Peninsula and in the Makhachkala and Fort-Shevchenko regions. Strong storms in the Caspian Sea (wind speed (V) ≥ 15 m / s) correspond to the types of north-west, south-east and north (or north-east) winds.

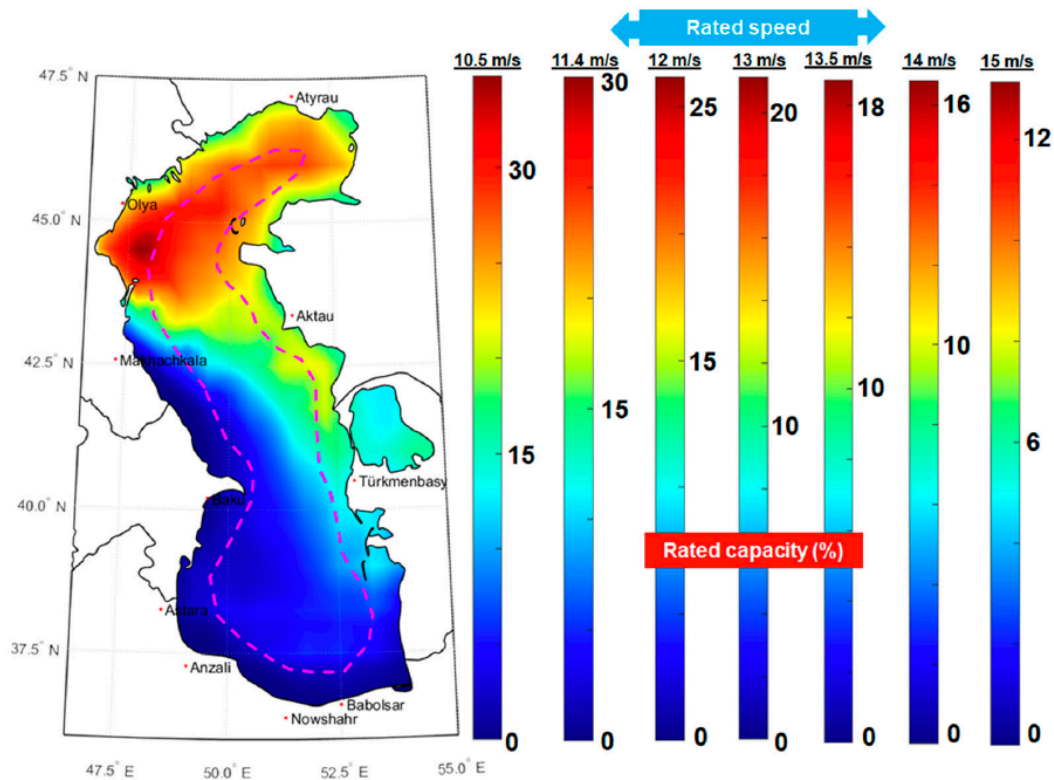


Figure 3. The rated capacity (%) reported for different rated wind speeds.

Regions of Caspian Sea are classified as follows:

1. Makhachkala - Derbent region. The wind speed is $V \geq 15$ m / s, which is about twice as much as in the western part of the Absheron region and is 40-50%. As in Region 3, all-directional winds are observed here, but south-east (30%) and north-west (25%) winds are also predominant. If the wind speed exceeds 16, 21 and 25 m / s, regardless of the direction, then their repetition is equal to 2.70, 0.40 and 0.06% respectively.
2. Fort - Shevchenko - Kandarli region. The number of days with wind speed $V \geq 15$ m / s is the same as in Makhachkala-Derbent regions. South-east (23%) and north-west (17%) winds prevail here. Higher speeds ($V \geq 25$ m / s) are characteristic of northern and north-western directions. Repetition of winds at speeds of more than 16, 21, 25 m / s is 2.4; 0.37 and 0.03% respectively.
3. Absheron region. The number of days with wind speed $V \geq 15$ m / s during the year depends on the orographic and nasal effects and is observed in 55-60 in the east of the Absheron peninsula and 115-145 in the west. The frequency of wind with a speed of more than 10 m / s in the Absheron region is 3.7%. The frequency of strong winds ($V \geq 15$ m / s) is 18%. Strong storms ($V \geq 25$ m / sec) can be observed in all points of Absheron region - from Ashagi bridge - (Nizkiy Pristan) to Sangi-Mugan island. North winds prevail in all seasons. Its average annual recurrence is 55% (north - 24, north-east - 13, north-west - 18%).

4. Krasnavodsk Black-Bosphorus-Gulf region (4). It differs very little from the northern regions due to wind conditions. The number of days with wind speeds exceeding 15 m / s is 40-50%. North (18%) and north-west (17%) winds are typical for the warm half of the year, and east (30%) winds are typical for the cold half. Strong storms are observed during north and northeast winds. North and north-west winds with a speed of more than 25 m / s are typical for all regions (1-4), south-east winds are typical only for Makhachkala-Derbent (1) region.
5. The western part of the South Caspian. According to the wind regime, this region is divided into 2 semi-regions: The first half of the region - north of the mouth of the Kura; The second half of the district is south of the mouth of the Kura. The first half of the region is dominated by north-east (26%) and north (14%) winds. The annual number of winds with a speed of more than 15 m / s is 60-70 days. The second half of the region is dominated by north-east (19%) and south-east (12%) and north-west (29%) winds. Their average annual number is relatively small (50-60 days).
6. The eastern part of the South Caspian region. This region is characterized by a decrease in the number of windy days (20-30 days) with a speed of more than 15 m/s. The frequency of strong winds with a speed of more than 15 m/s is slightly more than 11 days. North and north-east winds prevailed in this region. The highest speed (21-25 m / sec) is observed during north winds.

2.1.3 Storage tanks classifications

2.1.3.1 Vertical storage tanks characterization (API-620 and API-650)

As previously said, one of Campedel's observations is that storage tanks are the equipment most damaged by natural disasters. Owing to the vast volume of hazmat contained, the effects of an explosion with this form of equipment are usually very serious. This chapter examines vertical atmospheric tanks that operate in close proximity to atmospheric conditions as a result of this. The API-620 and API-650 standards were used to define and parameterize this category of equipment (American Petroleum Institute, 2013, 2020). And for petrochemical industry, these guidelines set minimum conditions for each of the storage tank components and functionalities. Establishes standards for the design, installation, testing, and repair of vertical storage tanks that operate under atmospheric conditions, among other things. The key components of a vertical storage tank are shown in Figure 4 based on API-650/620.

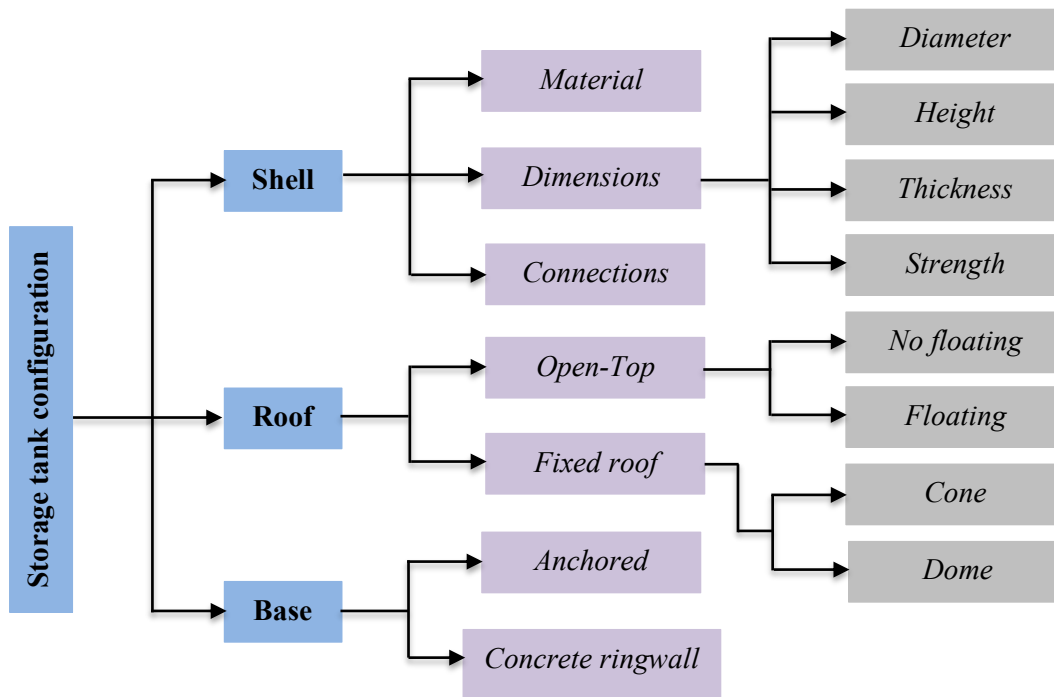


Figure 4. API-620 and API-650 standards are used to design a storage tank.

There is no easy way to categorize storage tanks using a single criterion. The equipment would be divided into three (3) key components in order to conduct a full sizing of the tank: the tank hull, the type of roof, and the type of foundation.

2.1.3.2 Storage tank shell

In the chemical and petrochemical industries, atmospheric reservoirs are most common kind of tank. The internal pressure of these tanks is normally marginally higher than ambient pressure, no more than 0.5 psig (3447.38 Pa) (Myers, 1997). The following specifications are necessary to parameterize the design of shell that will hold the stored fluid: shell content, number and type of connections, tank width, height, and thickness. The type of shell content is one of the most important factors in determining the tank's resistance; each material has its own yield and tensile strengths. API-650 suggests the following phrases in term of tank height and diameter to determine tank thickness (American Petroleum Institute, 2020):

- For the first course:

$$t_1 = \left(1.06 - \frac{0.0696D}{h} \sqrt{\frac{hG}{S_d}} \right) \left(\frac{4.9hDG}{S_d} \right) + CA \quad (2)$$

- For the second course:

$$t_2 = \begin{cases} t_1 \rightarrow \text{if } \frac{h_1}{(rt_1)^{0.5}} < 1.375 \\ t_{2a} \rightarrow \text{if } \frac{h_1}{(rt_1)^{0.5}} > 2.625 \\ t_{2a} + (t_1 - t_{2a}) \left[2.1 - \frac{h_1}{1.25(rt_1)^{0.5}} \right] \rightarrow \text{if } 1.375 \geq \frac{h_1}{(rt_1)^{0.5}} \geq 2.625 \end{cases} \quad (3)$$

- For upper courses:

$$t_i = \frac{4.9D \left(h - \frac{x}{1000} \right) G}{S_d} + CA \quad (4)$$

Where x is the distance between the variable design point and the course's bottom. (m).

Equations 2–4 can be used to characterize the tank's shell based on geometrical properties and the tank's material form.

2.1.3.3 Storage tank roof

Two roofs, a fixed roof and/or a floating roof, may be used to build a storage tank. The tanks may be opened at the top or closed by either a fixed roof, as seen in Figure 5:

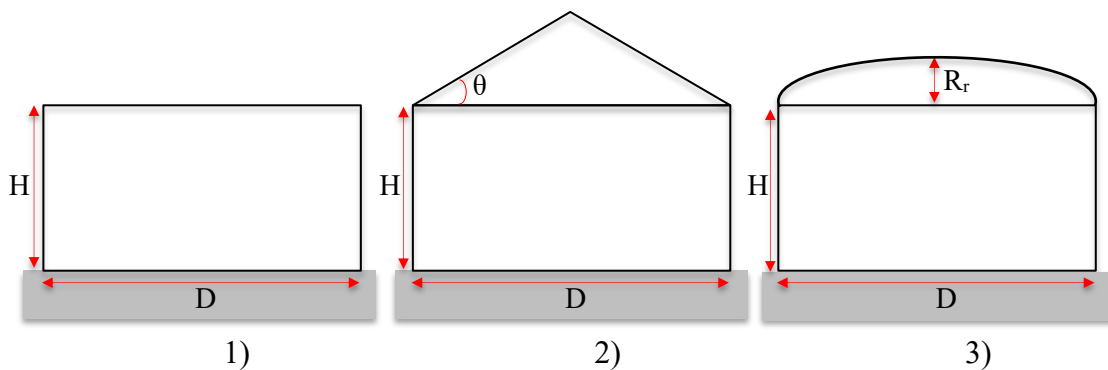


Figure 5. A storage tank's general configuration. 1) open-top tank, 2) cone-roof tank, 3) dome-roof tank

Cylindrical shells with a longitudinal axis of symmetry in the example of cone-roof tanks. The bottom is typically flat, and the top is shaped like a shallow cone. Even in very small-diameter tanks, cone-roof tanks generally have roof rafters and support columns (Figure 5 2) (Myers, 1997). The inclination angle of the roof is between 9.5° and 37° , per the API-650 (slope 2:12 to 9:12).

$$t_{rc} = \frac{D}{4.8 \sin(\theta)} \sqrt{\frac{\tau}{2.2}} + CA \quad (5)$$

where τ is a load combinations parameter. The nominal thickness of the cone roof is calculated using Equation 5.

Dome-roof tanks are identical to tanks with a cone roof, but their form is similar to that of an umbrella. These typically have a diameter of no more than 20 meters. These may be self-supporting structures, unlike tanks with a conical roof (Figure 5 3). The radius of the dome is between $0.8D$ and $1.2D$, as per API-650.

$$t_{rd} = \frac{R_r}{2.4} \sqrt{\frac{\tau}{2.2}} + CA \quad (6)$$

Where R_r is the roof radius (m). Equation 6 calculates the dome roof's nominal thickness.

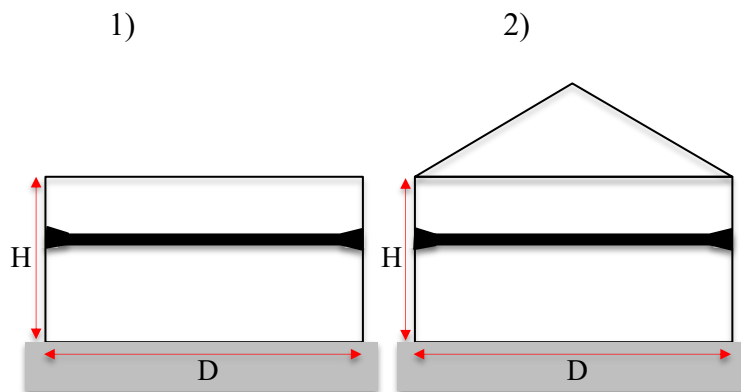


Figure 6. In a storage tank, there are two types of floating roofs: 1) external floating roofs and 2) internal floating roofs.

All of floating roofs are located inside of the storage tanks and are a cover that floats on top of the oil. This roof cover is a disk-shaped construction with enough buoyancy to keep the roof afloat under some situations. External floating roof (Figure 6-1) refers to tanks with a floating roof but no fixed roof; internal floating roof (Figure 6-2) refers to tanks with a floating roof but a fixed roof.

2.1.3.4 Storage tank base

The base of storage tanks has an extra resistance element. To prevent machinery displacement in the event of an external lateral load, a tank may be bolted or unanchored to the deck. It may also be constructed on a concrete ring that prevents the tank from collapsing into the ground on which it is constructed.

Figure 7 shows a detailed diagram of a storage tank's anchorage. The number of tank anchor bolts, their diameter, and the type of material are needed for studying the effects of wind gusts on storage tanks.

Possible unintended situations that may occur during the effect of the accident on the process equipment are investigated using the natural hazard classification and the structural structure of the storage tank. The following are the unintentional situations that were considered for this report.

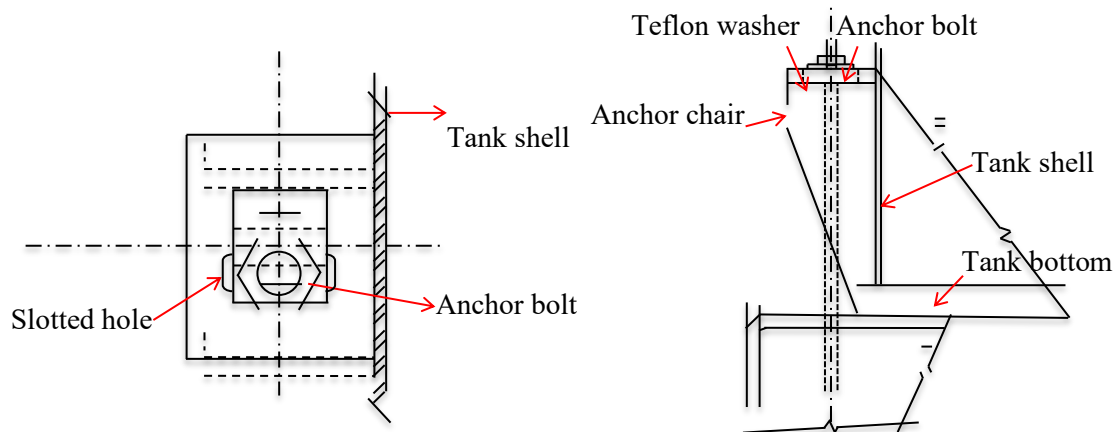


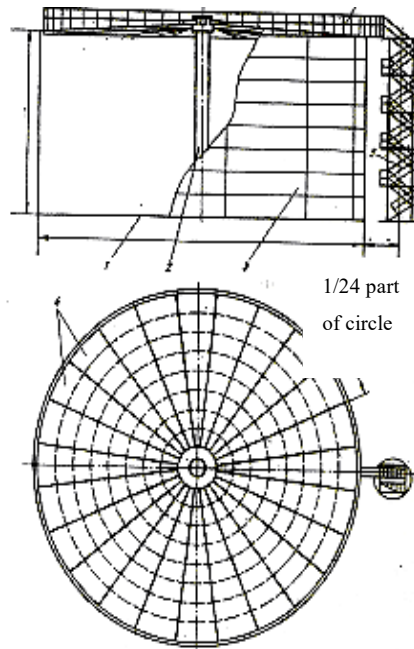
Figure 7. *Detail of a tank anchor*

2.1.4 Classification of oil storage tanks using in Azerbaijan.

Oil storage tanks meet the requirements of durability and longevity, as well as low evaporation losses. Depending on the material of oil tanks, they are made of reinforced concrete, steel, metal and non-metallic materials in various constructions. Steel oil tanks are subject to additional pressure in the gas phases: low (up to 2000Pa), high (up to 70,000Pa) and atmospheric pressure. According to the design, steel oil tanks are vertical cylindrical, horizontal cylindrical, drop-shaped and trench-type. Vertical cylindrical oil tanks are the most common and are mainly conical, spherical, pantone, floating lid.

2.1.4.1 Vertical cylindrical oil tanks. These tanks differ in the design and volume of the covers. The volumes of normal cylindrical oil tanks are: 100, 200, 300, 400, 500, 700, 1000, 2000, 3000, 5000, 10000, 20000, 30,000 and 50,000 m³. With the exception of oil tanks with a capacity of 50,000 m³, all remaining tanks are built by the industrial method. The 50,000 m³ oil tank is being built by both industrial and stratification methods. At present, large oil tanks (100,000, 150,000, 200,000 m³) are placed in the fleet of oil tanks abroad from Azerbaijan, which significantly reduces construction and installation costs and oil losses.

The disadvantage of 100,000 m³ oil tanks is that the thickness of its belts is reported to be 28-35 mm, which does not allow the belts to be rolled. It is convenient to build such oil tanks by the layer method. A vertical cylindrical oil tank with a capacity of 5000 m³ (Figure 8) consists mainly of a body, a bottom and a conical cover.



1- bottom; 2- central support; 3- body; 4 - cover wall; 5 - frost-type ladder; 6 - cover.

Figure 8 Vertical cylindrical oil tank with a capacity of 5000 m³.

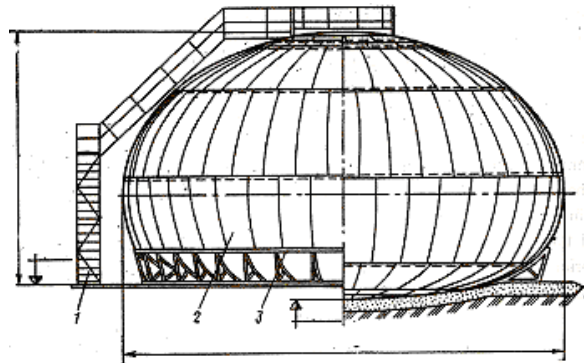
2-

The diameter of the tank is 22800 mm, the height of the body is 11920 mm, and the weight is 89231 kg. The bottom is installed in the form of a roll.

Table 3

Volume of tank, m ³	Actual sizes, mm		Optimal sizes, mm	
	Diameter, D	Height, H	Diameter, D	Height, H
1000	123330	8940	10430	11920
5000	22800	11920	20920	14900
10000	34200	11920	28500	17880
20000	45600	11920	39900	17880
30000	45600	17880	45600	17910
50000	60700	17880	60700	17910

2.1.4.2 Drop-shaped oil tanks. The tensile stress generated by the additional pressure is the same at all points of these tanks. The diameter of the drop-shaped oil tank (Figure 9) along the equator is 18500 mm, the distance to the highest point of the seat is 10850 mm, the thickness of the cover is 5-6 mm, the outer diameter of the support ring is 16494 mm, the inner diameter is 13364 mm, the width is 1665 mm, the layer thickness is 10 mm.



1- ladder; 2- trunk; 3- dib

Figure 9. Drop-shaped oil tank.

The support ring is made of 8–10 mm thick layer and has rigid ribs in the radius and direction of the ring. The number of ribs is 40. Inside the tank, the 8 mm thick rib extends from the edges of the bottom to the top of the support ring. In Azerbaijan, drop-shaped oil tanks are made of "St.3" martensitic steel. 64 tons of metal are used to make such an oil tank. 63.4% of this metal is in the tank body; 12.8% to the inner frame, 21.1% to the support part and 2.7% to the ladder, fence, etc. is spent.

2.1.4.3 Horizontal cylindrical oil tanks. These tanks are used in various sectors of the economy. In these types of tanks, the oil is usually stored under additional pressure (Figure 10). The optimal parameters of surface horizontal cylindrical oil tanks are given in Table ##.

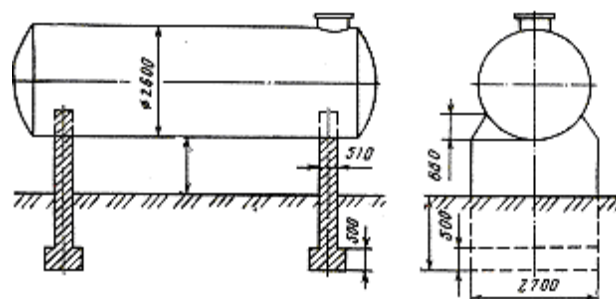


Figure 10. Horizontal cylindrical oil tank

Inside the tank, two diaphragms consisting of two angles and five intermediate stiffness rings are installed. The stiffness rings are welded to the body of the tank at an angle of $75 \div 50 \div 5$ mm and at a distance of

1.8 m from each other. The support rings of the diaphragm are made of a large angle of 120 ÷ 80 ÷ 8 mm and are welded to the body of the tank. The tank is placed on poles.

Table 4

Optimal parameters of horizontal cylindrical oil tanks

Nominal volume, m ³	Diameter, m	Length, m	Internal pressure, MPa
5	1,9	2	0,04
10	2,2	3,3	0,07
10	2,2	2,8	0,04
25	2,8	4,8	0,07
25	2,8	4,3	0,04
50	2,8	9,6	0,07
50	2,8	9,0	0,04
75	3,2	9,7	0,07
100	3,2	9,0	0,04
100	3,2	12,7	0,07
500	6,0	18,0	0,04
1000	6,0	35,8	0,02

2.2 Accidents scenario

Since the frequency of Natech events has increased in recent years, various authors have produced research, observations, and risk tools related to these types of events. The French Ministry of Sustainable Development conducted a report in 2008 to determine the distribution of natural phenomena across Europe, which resulted in significant human, social, and economic losses. Storms and floods are the natural disasters that most impact the majority of European countries, according to the findings of this report. Similar patterns can also be observed in other parts of the world. As a consequence of the increasing number and duration of natural disasters around the world. ARIA (Analyze, Recherche et Détails sur les Accidents), FACTS (Failure and Accidents Technical Information System), MHIDAS (the Major Hazard Incident Data Service), MARS (Major Accident Reporting System), and ICHEME (Institution of Chemical Engineers) are some of the key European sources where data on Natech incidents is collected. The NRC, on the other hand, is the most widely used database on the American continent (National Response Center).

Figure 11 presents the distribution of the records between the aforementioned databases (Campedel, 2008).

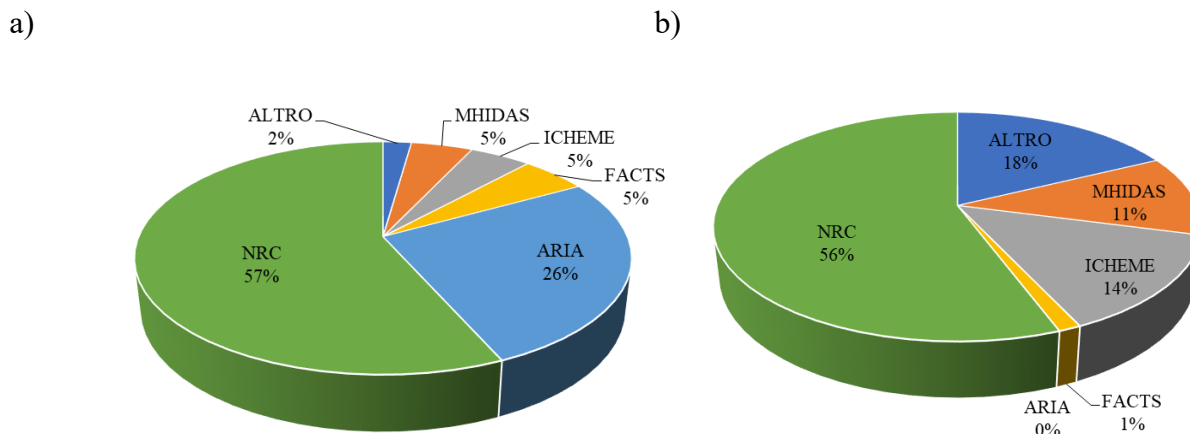


Figure 11. The following is a list of the Natech accident accidents that were discovered through a review of the available chemical accident databases: a) flood accidents (272), b) seismic accident (78) (Campedel, 2008)

Figure 12 indicates that when a Natech happens, hydrocarbons (oil, petrol, and gasoline) are the most commonly released compounds. Explosions, flames, and chemical dispersions are all possible outcomes of these compounds.

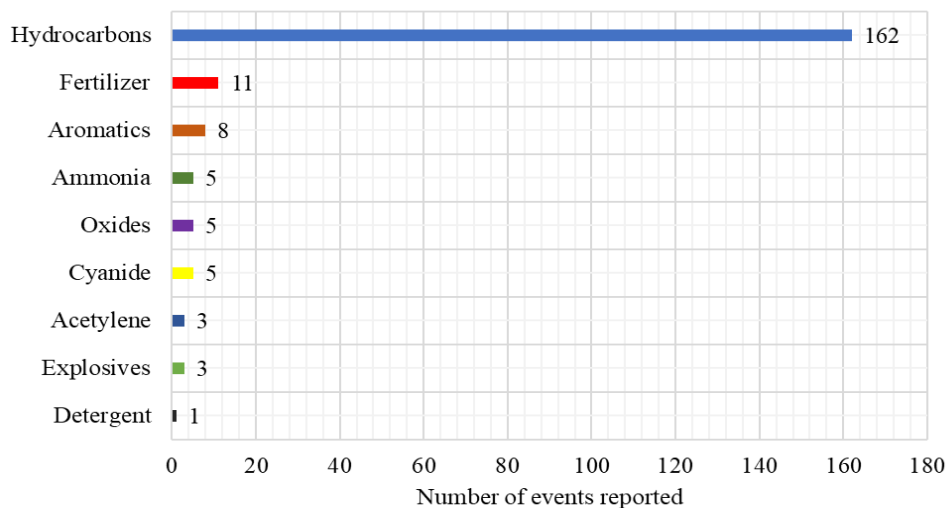


Figure 12. Common substances found in Natech accidents (Campedel, 2008)

2.2.1 Natural hazards

A natural hazard, according to Burton et al. (1978), involves human and systemic involvement. A physical occurrence is one that has no effect on people or buildings, so it is referred to as a natural event or anomaly rather than a natural hazard. When it affects those, who are vulnerable to it, it becomes a natural hazard.

Natural events that occur in densely populated or industrialized areas are dangerous occurrences that can result in a large number of deaths or incalculable property damage, leading to a natural disaster. As a result, natural disasters do not pose a threat to process safety in places where there are no humans or manufacturing facilities, and therefore would not cause a catastrophe. Natural disasters not only kill everything in their way, but they also cover vast areas and impact several targets at the same time.

Geophysical hazards: a) earthquakes, b) tsunamis, c) volcanic activity; meteorological hazards: a) tropical cyclones, b) extratropical storms, c) convective storms, d) hurricanes; hydrological hazards: a) floods b) mass movements; climatological hazards a) high temperatures, b) drought, c) forest fires. One of the main issues of the global industry sector in recent years has been the rise in the frequency of high-intensity natural disasters, owing to climate change impacts, as well as an increase in industrial exposure. The natural phenomena that most frequently impact the earth, as shown in Figure 13 (Munich RE, 2019).

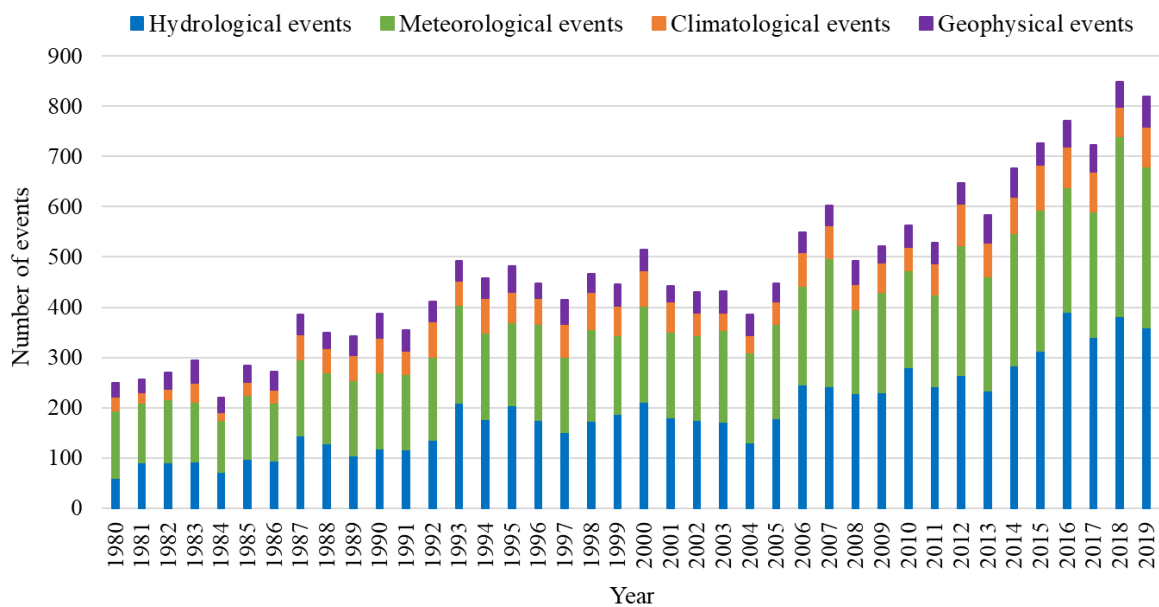


Figure 13. *Natural losses that have occurred around the world.*

Furthermore, as the incidence of natural disasters increases, so do the economic losses correlated with the damage caused by the events. And not just because the environment is subjected to more natural hazards, but also because their severity grows over time, increasing the potential for harm. Figure 14 (Munich RE, 2019) depicts a worldwide calculation of gross annual economic losses caused by all-natural hazards combined.

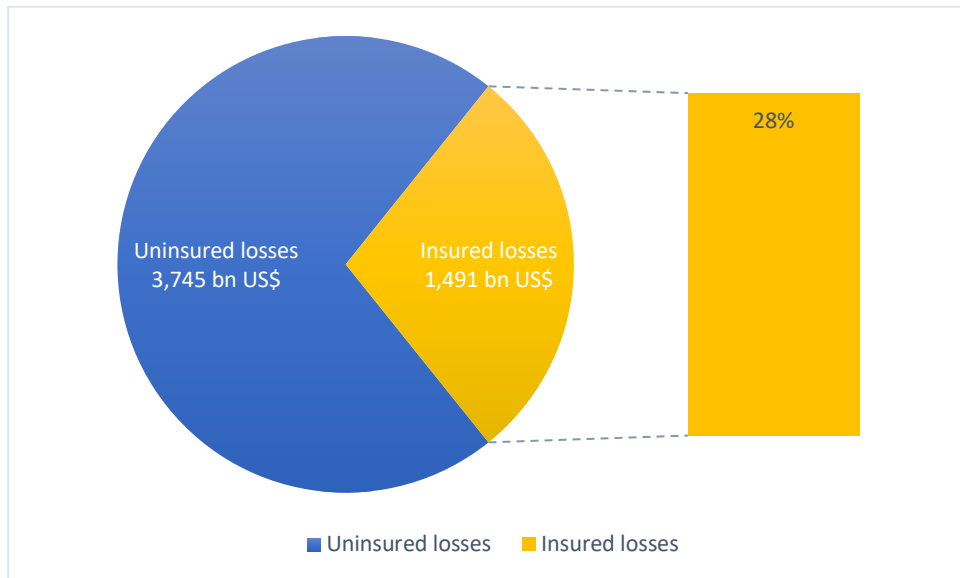


Figure 14. *Uninsured and insured losses worldwide* (Munich RE, 2019)

The cost of damages and repairs to private and public property (including the manufacturing sector), as well as victim assistance and reparation, disaster response, and environmental remediation, are all factored into the total value of economic losses. Since Natech incidents lead to these annual losses, a greater understanding of the risk mechanisms and threats due to industrial facilities, as well as their possible impacts and effects on their surroundings, would aid in reducing these losses.

It is necessary to classify natural events according to their frequency and intensity in order to assess the potential for harm. Equation (7) indicates that the frequency (1/year) of a natural disaster is the inverse of its return duration, which is the number of years it takes for a natural phenomenon of a given severity to occur (Antonioni et al., 2015).

$$f = \frac{1}{t_r} \quad (7)$$

2.2.2 Natech Risk

Different authors have built expertise for the study and management of the associated risks with Natech incidents, taking into consideration the significant threat posed by natural phenomena on industrial plants (Mesa-Gómez et al., 2020; Mesa-Gómez et al., 2021). The analysis of Natech events and their threats is driven by two approaches. First, there's a posteriori analysis, which entails defining facts that can be used to characterize an occurrence based on historical evidence or records from previous incidents. Second, there's a priori review, which entails evaluating potential accident situations and assessing the threats they pose (Villalba, 2016). Figure 15 depicts a timeline with models built for estimating the damages to a reservoir caused by various natural hazards (left side) and risk assessment methodologies associated with

Natech events (right side) (right side). For risk assessment, the methodologies discussed use damage models.

2.2.3 Storage tank accidents

Significant quantities of flammable and toxic chemicals are stored in storage tanks in refineries and chemical plants. A minor incident could result in a million-dollar property damage and a few times of production disruption. Litigation, stock depreciation, and business collapse are all possible outcomes of a major accident. In the last 50 years, trade unions and engineering societies such as the American Society of Civil Engineers (ASCE), the American Petroleum Institute (API), the American Institute of Chemical Engineers (AIChE), the American Society of Mechanical Engineers (ASME), and the National Fire Protection Association (NFPA) have all authored engineering specifications and regulations for the development, selection of materials, design, and safe maintenance of storage tanks and their supports (AIChE, 1988; 1993; API, 1988; 1990; ASME, 2004; NFPA, 1992; UL, 1986; 1987). Despite the fact that most businesses adhere to these requirements and guidelines in the design, construction, and service of tanks, accidents do happen. Learning from the experience is important for the safe functioning of storage tanks in the future. The following is a list of the causes of the 242 tank incidents that have occurred in the last 40 years. Dr. Kaoru Ishikawa (Ishikawa and Lu, 1985) invented the fishbone diagram (the cause-and-effect diagram) to summarize the effects and the factors that produce or lead to those effects.

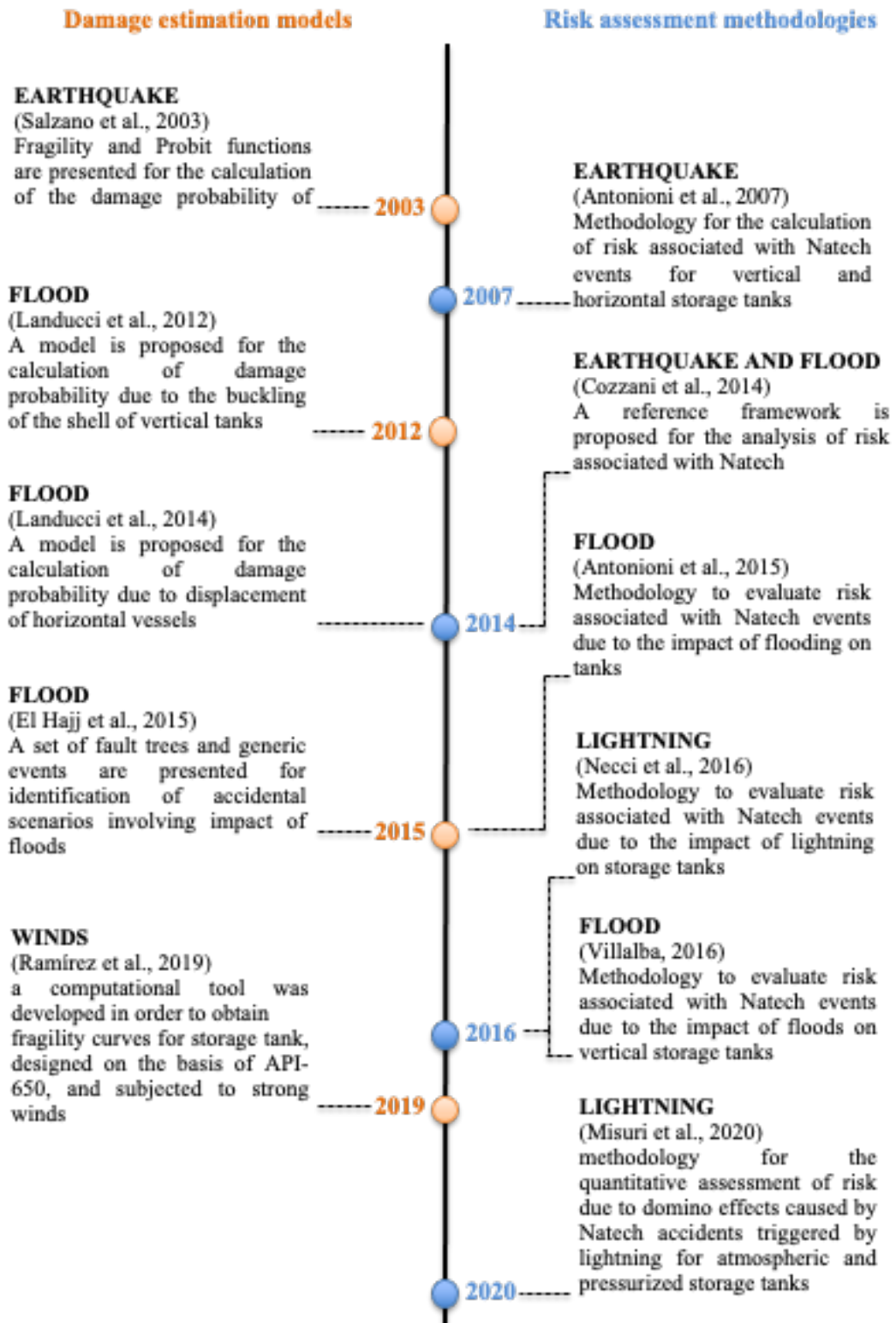


Figure 15 The state of the art for a categorical Natech case analysis (Antonioni et al., 2007, 2015; Cozzani et al., 2014; El Hajj et al., 2015; Landucci et al., 2012, 2014; Misuri et al., 2020; Necci et al., 2016; Ramírez Olivar et al., 2020; Salzano et al., 2003; Villalba, 2016)

According to the details obtained from 242 tank accidents, 114 happened in North America, 72 in Asia, and 38 in Europe (Figure 16).

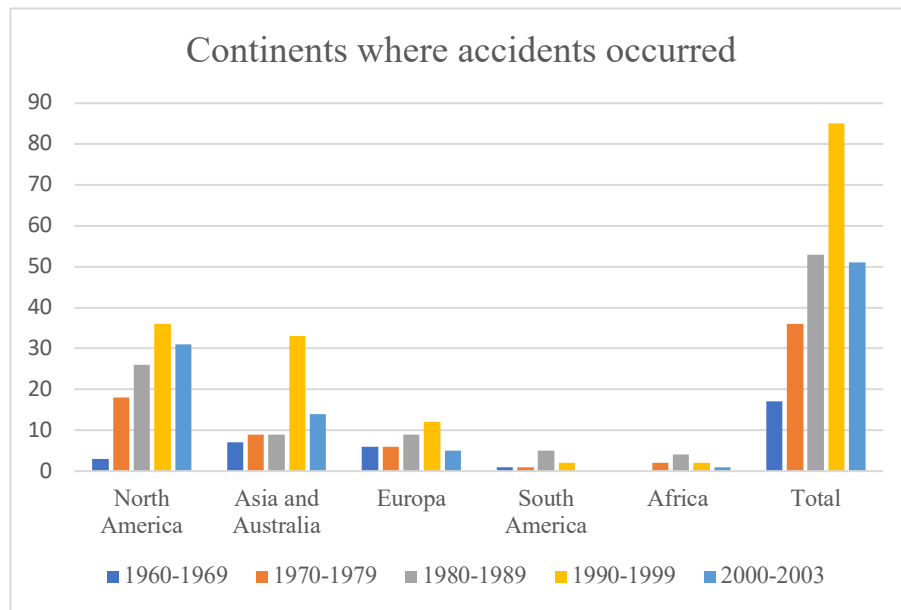


Figure 16. *Continents where accidents occurred*

Since accident data is easily available in the United States, 105 injuries were investigated. Accidents occurred at petroleum industry, as seen in Figure 17, with 116 accidents (47.9 percent). Terminals and pumping stations were the second most commonly involved place (64 cases, 26.4 percent). Just 25.7 percent of incidents occurred in petrochemical plants (12.8%), oil fields (2.5%), and other forms of manufacturing facilities (10.1%), such as power plants, gas plants, pipelines, fertilizer plants, and so on.

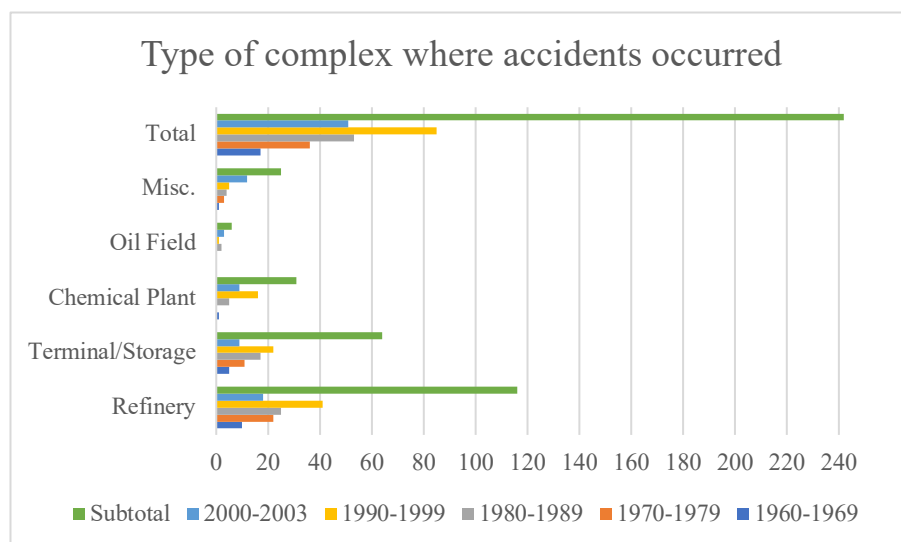


Figure 17. *Type of complex where accidents occurred*

The main contents were crude oil, gasoline, and oil products such as fuel oil, diesel, and so on (Figure 18). The most common model was an atmospheric exterior floating roof tank, with an atmospheric cone roof

tank coming in second. Both types were widely used to store crude oil, gasoline, and diesel fuel (Figure 19).

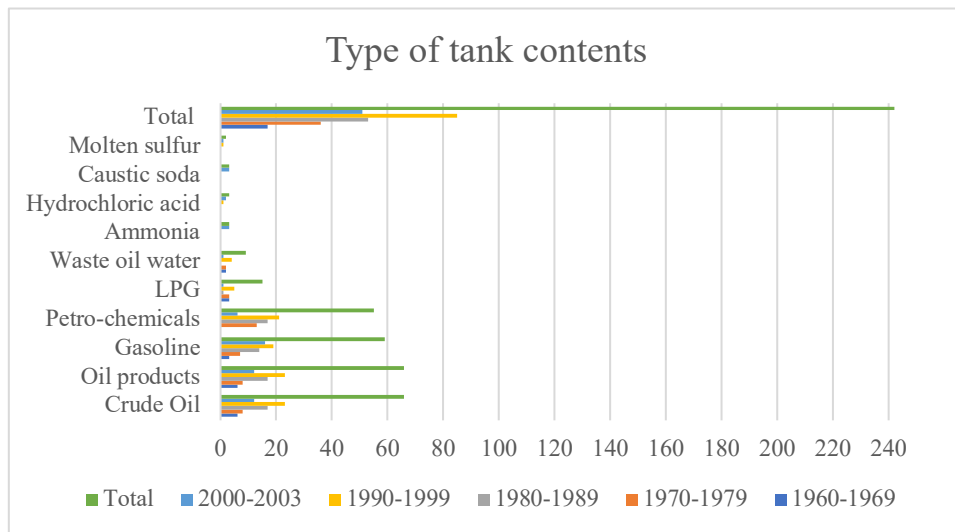


Figure 18. *Type of tank contents*

Figure 20 shows that fire was the most common form of loss, with 145 cases, and explosion was the second most common type of loss, with 61 cases. Together, fire and explosion accounted for 85 percent of all incidents. The third and fourth most common incidents were oil spills and hazardous gas/liquid releases, respectively. The worker's fall and the tank body imbalance just happened a few times. Property losses were uncommonly recorded, and data was difficult to come by.

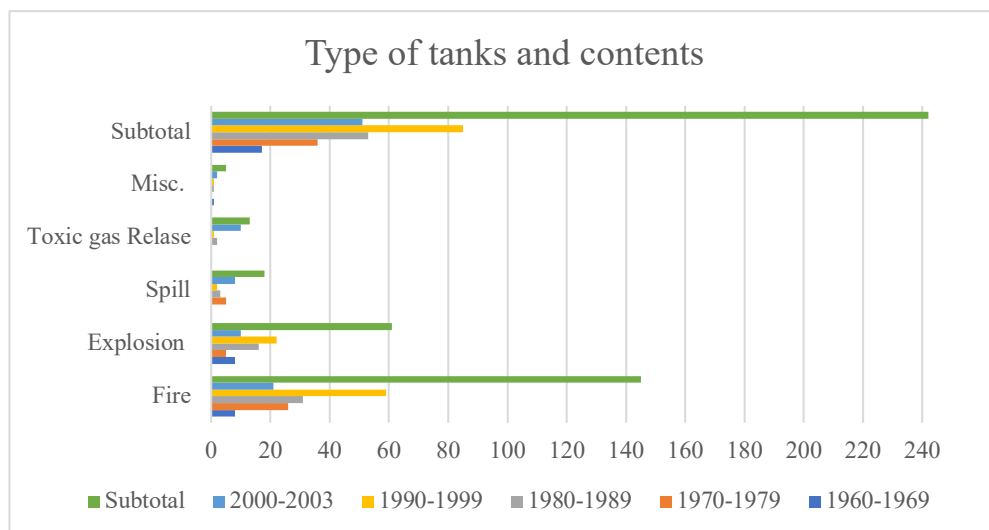


Figure 19. *Type of tanks and contents*

According to the report, lightning was the most common cause of accident, and maintenance fault was the second most common cause.

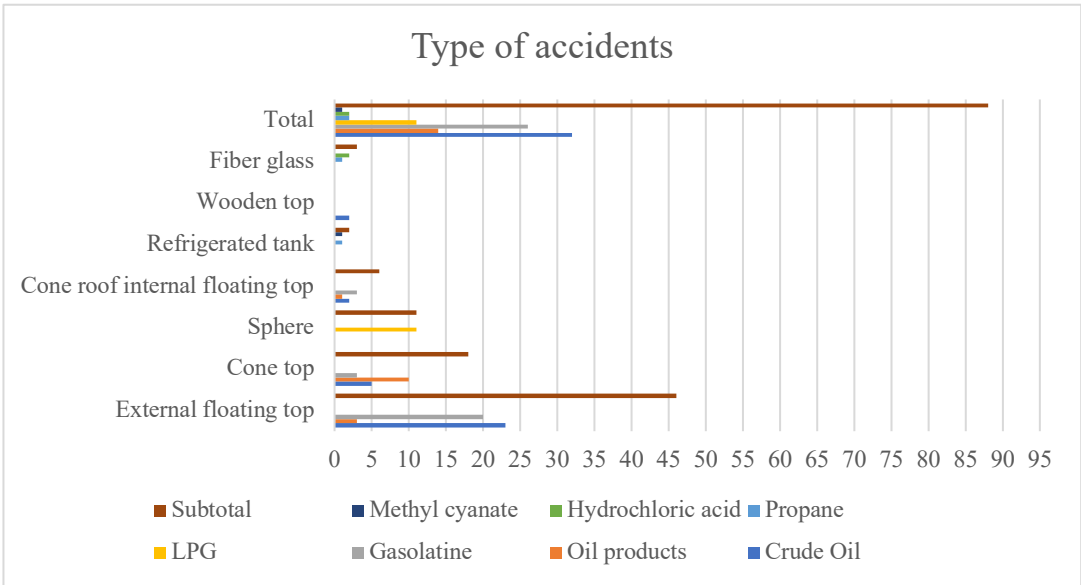


Figure 20. Type of accidents

Operational malfunction, system breakdown, sabotage, crack and rupture, leak and line rupture, static electricity, open flames, and so on were among the remaining causes. A fishbone diagram, as shown in Figure 21, was created to explain causes and effects. A fishbone diagram, as seen in Figure 22, was also created to improve in accident prevention.

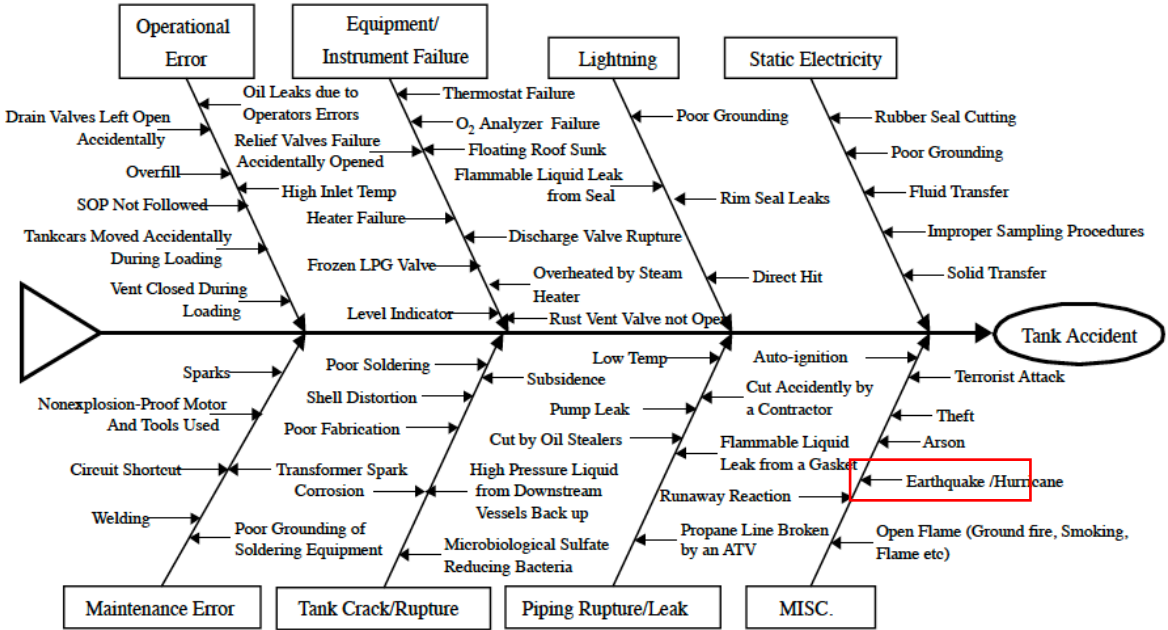


Figure 21. Fishbone diagram of accident causes.

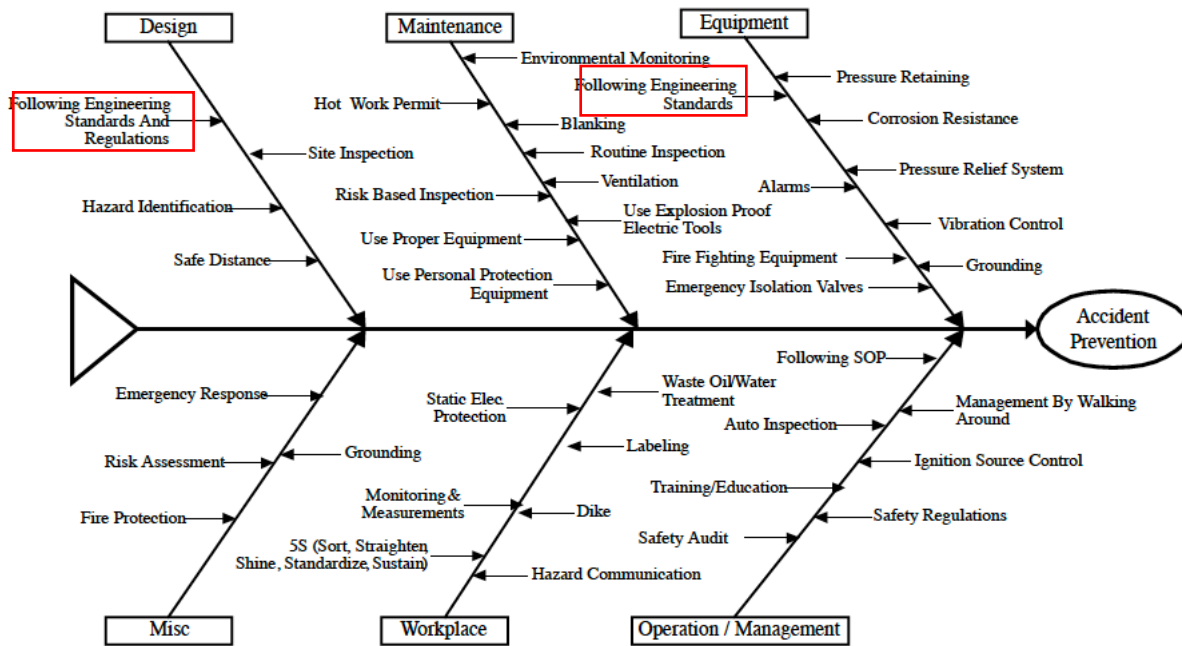


Figure 22. Fishbone diagram of accident prevention.

In the last 40 years, data on 242 tank incidents in industrial facilities was analyzed. A fishbone diagram was used to express the causes and contributing failures that contributed to the incidents in a systematic manner. The majority of those tank accidents could have been avoided with good engineering in design, building, repair, and service, as well as a safety management program that was introduced and enforced.

2.2.4 Definition of potential accidental scenarios

The incident tree approach is used to describe the potential final unintended situations that can be caused by strong winds on a vertical storage tank. ARAMIS (Salvi et al., 2002) suggests a method for developing event trees that is tailored to Natech events triggered by the natural phenomenon described. The events tree's goal is to classify the potential outcomes of a crucial occurrence, also known as a CE, which normally represents a system failure or an external failure. The series of events or security features that occur after the initiating event is then specified and must be resolved in order to achieve a specific outcome. Secondary critical events (SCE) are these kinds of events, while final events or main events (FE) are the events that occur at the conclusion of each branch (Ocampo, 2016). The major effects caused by secondary events capable of influencing humans, systems, and the atmosphere are referred to as final events. An event tree and its components are depicted in Figure 23.

The effect of a wind forces on a storage tank is the selected critical event (CE) until the event tree has been identified. The wind speed is the defining characteristic of a wind load. Table 1 shows the four (4) different types of wind loads that have been developed. Secondary critical events (SCE) are chosen based on the effects of a natural disaster on a vertical storage tank. Some authors (Campedel, 2008; Cozzani et al., 2010) introduce a historical data study in which she described various forms of structural failure that

storage tanks can sustain during natural disasters. Damage modes, failure modes related to damage, and release modes were defined as three (3) categories of secondary critical events based on these analyses (LOC).

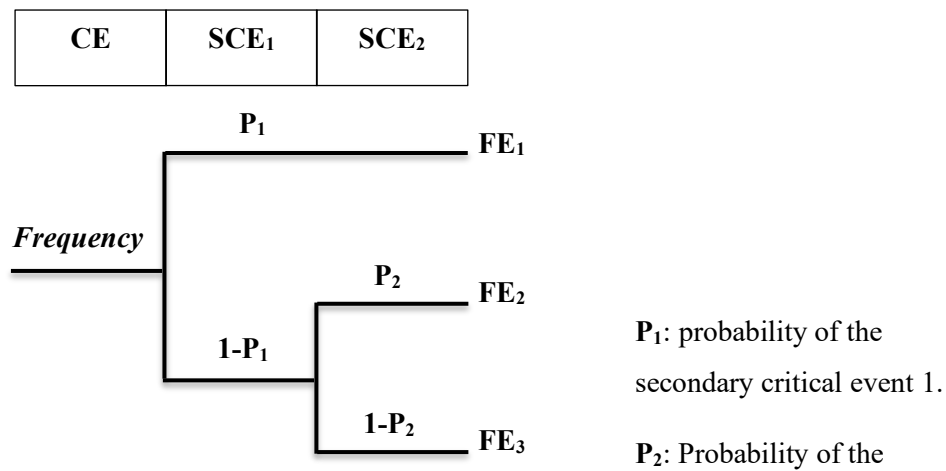


Figure 23. Structural event tree (Ocampo, 2016)

Shell buckling, displacement or slipping, floatation, overturning, and debris effect are also possible injury types for a storage tank. It's worth noting that not all destruction modes apply to all types of natural disasters. Buckling, overturning, and debris impact are now the most frequent effects of strong winds. The forms of damage caused by strong winds are mentioned in Table 2 along with their classification. When a strong wind loads strikes a storage tank, five (5) separate failure modes may occur as a result of the damage: the collapse of the foundation, complete failure of the connection, partial collapse of the connection, failure of the tank's roof, and breach of the hull. Figure 24 depicts a generic event tree for determining the outcomes of a Natech occurrence in storage tanks.

Natural hazard	Damage mode	Failure mode	Release mode
		Without affectation	
	Buckling	Collapse of the structure	Mode 1
Hazard intensity	Rigid sliding	Total connection failure	Mode 2
	Overturning	Partial connection failure	Mode 3

Figure 24. The series of events that occurred as a result of the effects of a natural disaster on vertical storage tanks is shown in this event tree.

Figure 25 depicts the event tree for determining the effects or final unintended scenarios (FE) associated with the effect of a wind load, and includes the elements discussed previously.

The lack of hazardous material containment occurs as one of the potential failure types occurs. Three (3) release modes have been developed for this secondary critical case, which will be part of the spill volume estimation process and are dependent on the failure typology.

For various types of process equipment, several recommendations and international standards have been developed (National Institute of Public Health and the Environment (RIVM), 2009; Uijt de Haag & Ale, 1999; van den Bosch & Weterings, 2005).

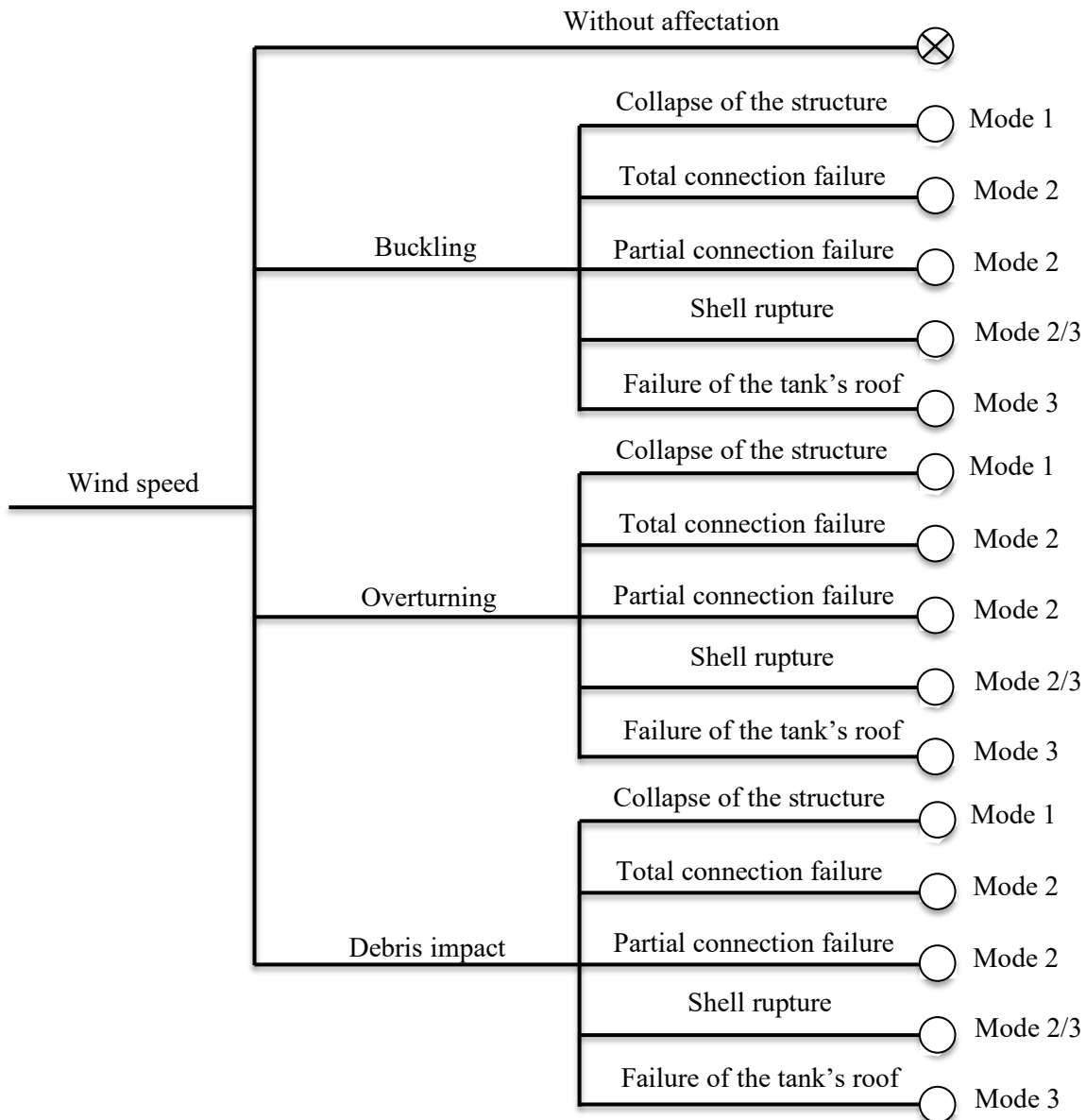


Figure 25. An event tree is used to determine the sequence of events that occur when a storage tank is affected by a wind load, based on the wind speed.

The following are the release types for atmospheric storage tanks based on these research:

- **Release Mode 1:** The entire contents are released at once.
- **Release Mode 2:** The entire contents are released in a steady and persistent stream over the course of 10 minutes.
- **Release Mode 3:** Continuous release from a cavity with a diameter of 10 mm effective diameter.

2.2.5 Analyses of structural and natural hazards

As previously stated, a natural hazard can cause harm to a storage tank as a result of its solicitation. The situation to be analyzed is depicted in Figure 26 as a plain outline. An severe natural phenomenon may produce an external load or solicitation (by friction or movement) of such severity that, when affecting some form of structure, the solicitation can surpass the resistance force with which it was engineered, causing structural harm.

Shell buckling, tank sliding or floating, damages to tank base, overturning, sediment effects, pipe detachment, and damage to the bottom plate by buckling due to uplifting are among the most frequent damages inflicted by a natural disaster on a tank.

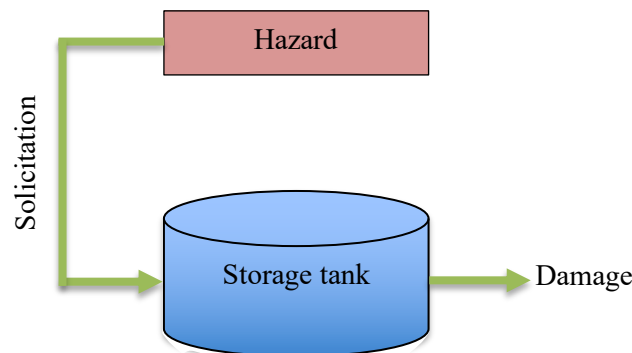


Figure 26. Damage as a result of natural hazard

Once the potential types of damage which will be assessed for each natural occurrence have been established, the load imposed for each form of damage should really be quantified. The mathematical models suggested by various writers to calculate the probability of various forms of damage are discussed in the following pages.

Table 5.

Damage classifications occurred by strong winds

Type of damage	Solicitation	Storage tanks resistance
Buckling	Wind pressure (q_{eq})	Resistance pressure (P_r)
Overturning	Stability factor (J)	-
Debris impact	Depth penetration (D_p) Impact force (F_i)	Thickness (t) Resistance force (F_r)

3. Materials and methods

In the following chapter, the material and methods used to achieve the results are presented. In the first part, the type of impact of strong winds on storage tanks are described related to the international standards. In the second part, the procedure followed to define and individuate method based on local standard used in Azerbaijan. The purpose is to use and compare different approaches.

3.1 Storage tanks damage by strong winds

The illustration shown below can be used to estimate the damage on a storage tank caused by strong winds. Figure 27 depicts the various forms of damage that strong wind speeds can do to a storage tank.

Cylindrical shaped storage tanks are structures capable of storing vast volumes of various materials such as crude, gasoline, and chemicals. They are welded, with very thin walls and large diameters and heights. The buckling of the walls due to the external pressure applied by the wind and the damage to the tank shell due to the effects of bullets pulled by the wind are the forms of damage examined in this study.

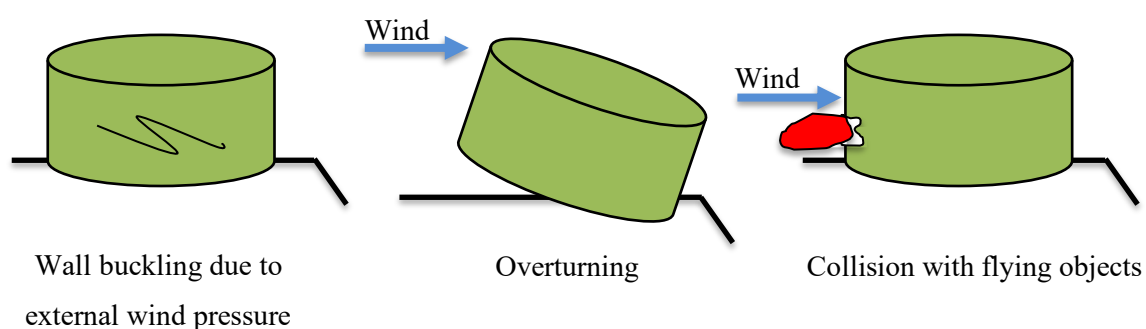


Figure 27. Types of damage to a storage tank exposed to high wind speeds

3.1.1 Shell buckling

When the tanks are empty or partly loaded, buckling of the shell causes damage (Uematsu et al., 2014; Zhao & Lin, 2014). This is also why, in the majority of situations, a mistake will result in a significant loss of financial and human capital but just a minor hazmat leak (Maraveas et al., 2015).

Figure 28 represents the pressure equilibrium over the storage tank, between the tank's resistance pressure and the wind outward pressure working over the tank, using the same technique as for buckling of tank shells due to flood.

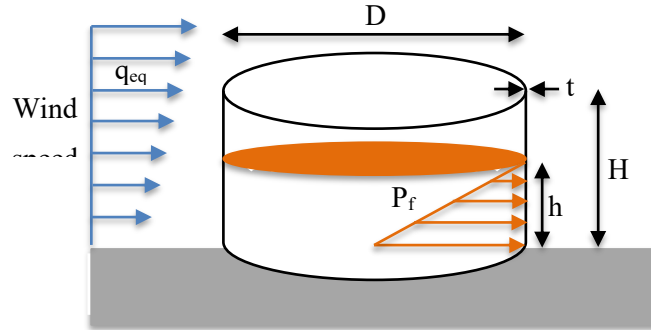


Figure 28. Scheme of the load-resistance forces assumed for wind-induced shell buckling are represented

The resistance pressures are given by equation 8, which is the sum of the pressure from the stored fluid (equation 9) and the material resistance pressure of the tank (equation 10). (Timoshenko & Gere, 2012). The above is determined by the tank's mechanical properties.

$$P_r = P_f + P_{cr} \quad (8)$$

$$P_f = \rho_f g h = \rho_f g H \Phi \quad (9)$$

$$P_{cr} = \frac{2Et}{D} \left(\frac{1}{(n^2 - 1) \left(1 + \left(\frac{2nH}{\pi D} \right)^2 \right)} + \frac{t^2}{3D^2(1 - \nu^2)} \left(n^2 - 1 + \frac{2n^2 - 1 - \nu}{1 + \left(\frac{2nH}{\pi D} \right)} \right) \right) \quad (10)$$

Furthermore, the formula for calculating wind pressure considers the sort of exposure of the affected system, according to international standards such as the American Petroleum Institute (API-650), American Society of Civil Engineers (ASCE-7), and European Standard (EN 1991-1-4 and EN1993-1-6). The design wind pressure is defined by the following phrases (American Petroleum Institute, 2020; American Society of Civil Engineers, 2017; European Committee for Standardization, 2005):

The velocity pressure q_z is calculated using Equation 11 at height z :

$$q_z = 0.00256 K_z K_{zt} K_d V^2 I G_s \left[\frac{lb}{ft^2} \right] \quad (11a)$$

$$q_z = 0.613 K_z K_{zt} K_d V^2 I G_s \left[\frac{N}{m^2} = Pa \right] \quad (11b)$$

Where:

- K_z is the velocity pressure impact coefficient (1.04 is used for open terrain exposure C at 12 m height),
- K_{zt} is the topographic factor (1.0 is used for all structures (exception is those on isolated hills or escarpments)),
- K_d is the wind directionality factor (0.95 is used for round tanks),
- V is the 3 sec gust wind speed at 10 m for open terrain exposure (exposure C) (mph or m/s),
- I is an importance factor (1.0 is used for category II structures),
- G is the gust factor (0.85 for exposure C).

The wind load or wind design pressure p (Pa) on the system surfaces over a storage tank is calculated using Equation 12 (Uematsu et al., 2014; Zhao & Lin, 2014):

$$p = C_p q_z \quad (12)$$

The wind pressure coefficient is denoted by C_p . It generally varies both around the diameter and the height of cylindrical tanks. Zhao & Lin (2014) discovered that the difference in height is less pronounced than the difference in diameter. As a result, the presumption is that pressure coefficient difference is constant along the height and only varies with longitude (see Figure 29). Several scholars and architecture codes have suggested an expression (Equation 13) based on Fourier series decomposition to approximate wind pressure coefficients. The representative Fourier coefficients suggested by some authors (Zhao & Lin, 2014) are shown in Table 5:

$$C_p(\theta) = \sum_{i=0}^m a_i \cos(i\theta) \quad (13)$$

where θ is the longitude is measured based on windward, and a_i is the Fourier's coefficient.

Table 6.

Different authors have proposed different Fourier coefficients for tanks with similar roofs.

Parameter	Author			
	Greiner	Rish	ACI-334	EN 1993-4-1
α_0	-0.65	-0.387	-0.2636	$-0.54+0.16(D/H)$
α_1	0.37	0.338	0.3419	$0.28+0.04(D/H)$
α_2	0.84	0.533	0.5418	$1.04+0.20(D/H)$
α_3	0.54	0.471	0.3872	$0.36+0.05(D/H)$
α_4	-0.03	0.166	0.0525	$-0.14+0.05(D/H)$
α_5	-0.07	-0.066	-0.0771	
α_6		-0.055	-0.0039	
α_7			0.0341	

The Fourier parameters in Table 6 are for the closed-top tanks, so no wind internal pressure is taken into account. To account for internal suction in tanks with an open top, a uniform negative wind pressure factor should be used, as seen in equation (14).

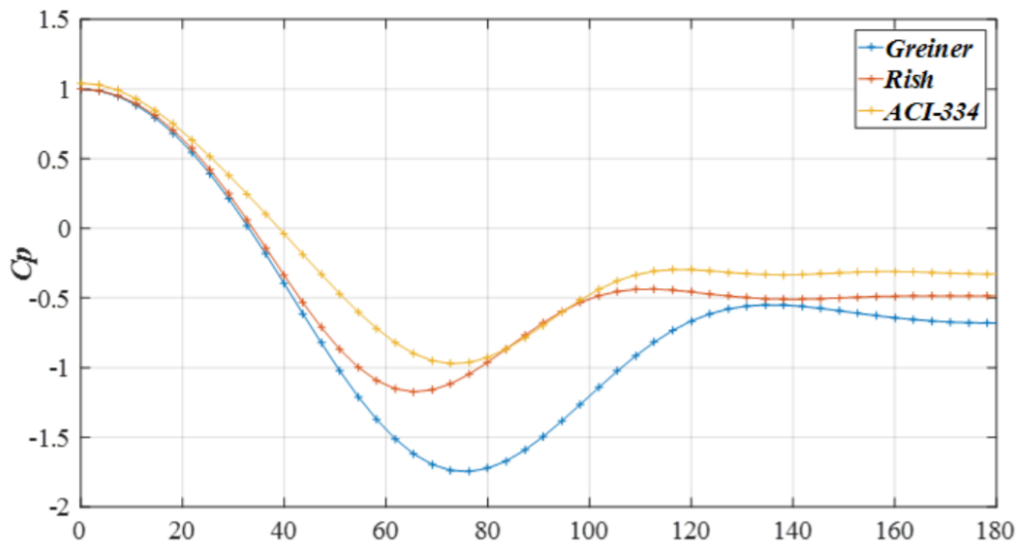


Figure 29. Wind pressure coefficients at extremes around the diameter of cylinders

$$C_p = \begin{cases} -0.8 \rightarrow \frac{H}{D} \geq 2 \\ -0.5 \rightarrow \frac{H}{D} \leq 1 \end{cases} \quad (14)$$

For shell buckling configuration, the non-uniform distribution of pressure p caused by external wind loading on cylindrical tanks may be replaced by an analogous uniform external pressure q_{eq} (Pa), as seen in Figure 30 (European committee for standardization, 2005), calculated using Equation 15:

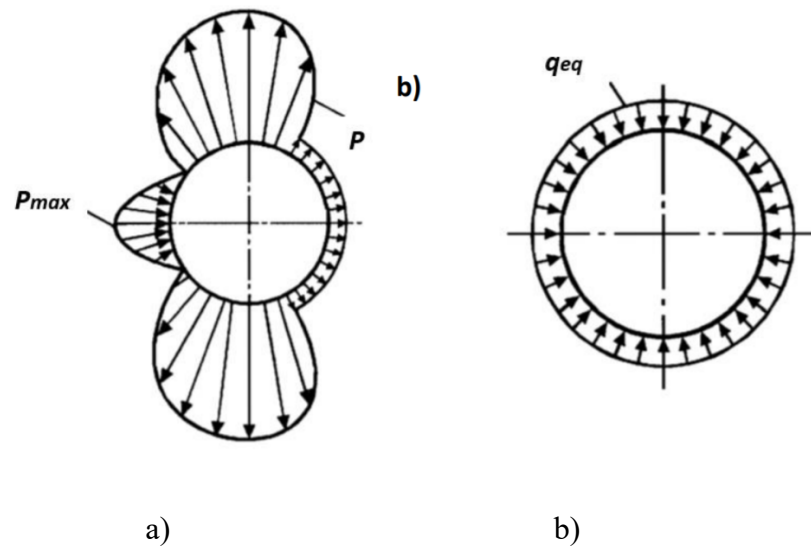


Figure 30. a) wind pressure distribution around the circumference of the shell, b) axially symmetric pressure distribution around the diameter of the shell (European committee for standardization, 2005)

$$q_{eq} = k_w p_{max} \quad (15)$$

where p_{max} is the maximum non-uniform pressure (Pa).

$$k_w = 0.46 \left(1 + 0.1 \sqrt{\frac{(C_{\theta} r)}{(\omega t)}} \right) \quad (16)$$

Figure 31 illustrates the non-uniform wind pressure profile for various wind speeds. The 0° angle refers to the wind direction. The related uniform external equivalent pressures are shown in Table 6.

Table 7.

Equivalent axisymmetric pressure at different wind velocities

Wind speed (mph)	q_{eq} (Pa)
75	0.7135
125	1.9820
175	3.8846
225	6.4215

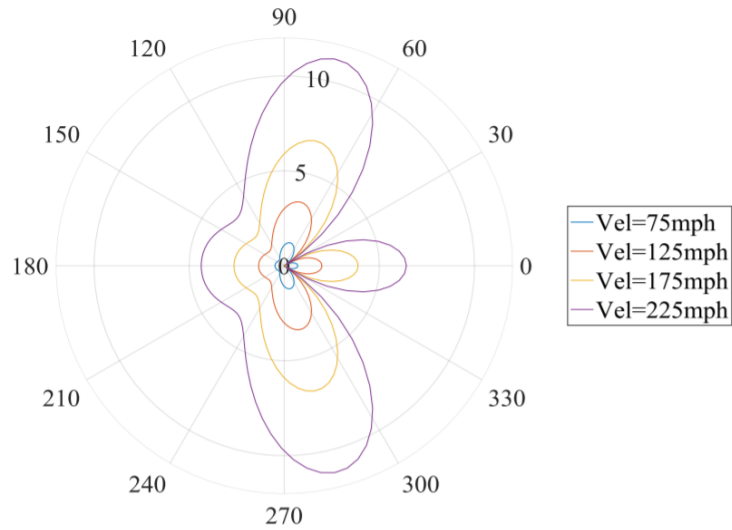


Figure 31. *Wind pressure distribution around shell circumference at different velocities*

As the tank is subjected to strong winds, the equilibrium between the wind loads acting on the tank (Equation 15) and the tank's resistance pressure (Equation 8) determines whether the machinery will be damaged by buckling or discoloration of its shell (Equation 17).

$$Damage = \begin{cases} \text{if } q_{eq} - P_r > 0 & \text{Buckling} \\ \text{if } q_{eq} - P_r \leq 0 & \text{No buckling} \end{cases} \quad (17)$$

3.1.2 Overturning

Hurricane Katrina, which created winds of up to 280 km/h and had the capacity to overturn a tank located onshore, is one of the most recent examples where international organizations have gathered knowledge about storage tanks impacted by excessive wind sources. This form of injury, according to some reports, is the least likely to occur, and when it does, the tank must be empty and without anchoring. The API-650 standard, on the other hand, specifies different stability requirements for a given wind load.

The harm incurred by overturning is discussed in this chapter for storage tanks that are not anchored to the bottom. The API-650 standard establishes stability requirements for tanks that are not anchored, as seen in Figure 32.

Equation 18-19 represents the stability requirement for a non-anchored tank overturning due to an outward wind load:

$$0.6M_w + M_{pi} < \frac{M_{DL}}{1.5} + M_{DLR} \rightarrow F_{o1} < F_{r1} \quad (18)$$

$$M_w + F_p(M_{pi}) < \frac{(M_{DL} + M_F)}{2} + M_{DLR} \rightarrow F_{o2} < F_{r2} \quad (19)$$

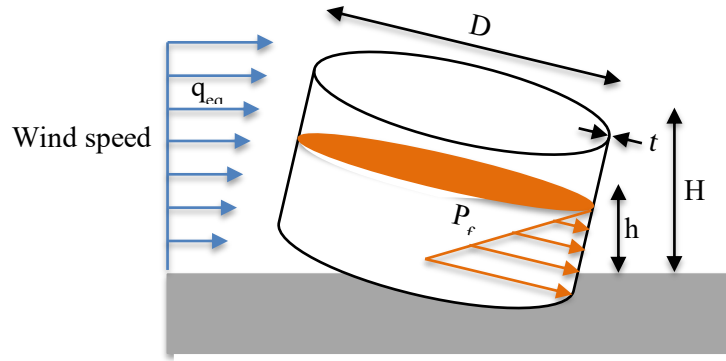


Figure 32. Scheme of load-resistance forces assumed the overturning by a wind load

Equation 17-18 will be used to decide whether the equipment will be damaged by overturning by establishing a relationship between the overturning forces F_{oi} generated by the wind on the tank at the time of being impacted by excessive winds and the resistance force of the tank F_{ri} .

$$Damage = \begin{cases} \text{if } F_{o1} - F_{r1} > 0 \text{ and } F_{o2} - F_{r2} > 0 & \text{Overturn} \\ \text{If } F_{o1} - F_{r1} \leq 0 \text{ or } F_{o2} - F_{r2} \leq 0 & \text{No overturn} \end{cases} \quad (20)$$

3.1.3 Impact of debris

Hurricanes and tornadoes have a high potential for destruction, especially when they have a long period of activity. When a building is destroyed, the waste created by the demolition becomes rubble or airborne missiles, which have the ability to collide with other structures and do significant damage (Pathirana et al., 2017). Since the area affected by harmful winds is so large, numerous buildings may be exposed to the impact of multiple debris, causing a domino effect on other structures.

Extreme winds have the potential to drag objects as they move. These artifacts pose a threat to a storage tank's integrity. The wind will bear enough force to destroy the components of a storage tank if an object is pulled by it. A combination of forces on the debris, which varies depending on the debris properties and wind conditions, is used to measure the force of impact of an object pushed by the wind.

As seen in Figure 33, an object pulled by the wind has a force that is proportional to the wind speed and would be compared to the tank's resistance force to determine potential impact. Salzano & Basco (2015)

suggest a new approach for assessing the susceptibility of a storage tank based on the magnitude of the impact (determined by Johnson's number J') and the extent of penetration (hp) caused by the impact.

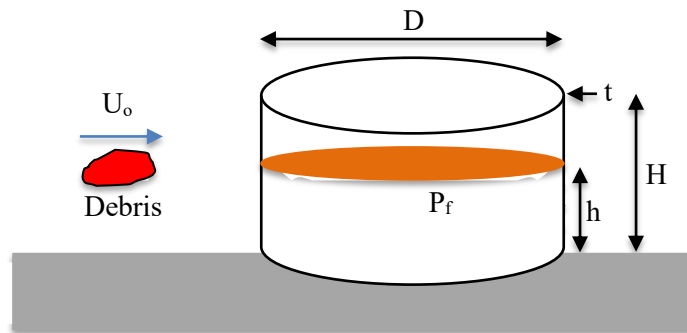


Figure 33. Scheme of load-resistance forces assumed for the effect of debris drag by the wind

The specifications and knowledge of the impact speed U_0 , the process equipment and the impact object are all linked in this technique. Johnson's number is used in impact dynamics to assess the magnitude of an impact on a continuum filled impetuously and impinged by the preliminary velocity pulse, and it can be calculated using Equation 21.

$$J' = \frac{U_0^2 M}{\sigma_D t r_p^2} \quad (21)$$

The spectrum of Johnson's number values, as well as the related regimes, are shown in Table 8. Johnson's number has been updated in (Lees, 2004) to measure the damage caused by the influence of an item in a storage tank:

Table 8.

Damage threshold values for Johnson's damage number J' (Salzano & Basco, 2015)

J	Regime	Probability of damage
1×10^{-3}	Quasi-static elastic	0
1×10^{-2}	Moderate plastic behavior	0.1
$1 \times 10^{+1}$	Extensive plastic deformation	0.5

Lin et al. (2005), on the other hand, suggested a technique for assessing the likelihood of moving objects pulled by the wind affecting urban buildings. The technique suggested by Lin is applied to a vertical storage tank. The impact force F_{ob} (N), which can be determined from the physical properties of the

material and the impact velocity, Equation 22, can determine whether an object will buckle or penetrated a storage tank.

$$F_{ob} = \frac{1}{2} \rho_w U_0^2 A_p C_F \quad (22)$$

where ρ_w is the wind density (kg/m^3), A_p debris area (m^2), and C_F is an aerodynamic force coefficient. Equation 22 refers to debris that is not fixed to the earth, allowing the material to be pushed and raised by the wind as the gravity of the debris exceeds the force of gravity ($F_i > Mg$). Equation 23 can be used to calculate the speed at which debris takes off. Since $M_g = A_p h \rho_p g$.

$$U_0^2 = \frac{2h\rho_p g I}{\rho_w C_F} \quad (23)$$

where I is a fixed strength integrity parameter, calculated as the ratio between the wind force required to overcome the friction force, divided by debris weight.

Finally, after the tank has been affected by debris, measuring the penetration depth h_p (m) of an object from its impact parameters is a practicable and practical way to confirm Johnson's damage figure. It should be remembered that in the case of industrial collisions, the penetration depth of a fragment or debris is a critical criterion for determining whether or not industrial machinery has lost its containment. If h_p reaches the thickness of the affected devices, the accumulated hazmat would be released unintentionally. Lee's textbook describes a simpler method for calculating h_p in terms of minimal thickness (Lees, 2004).

$$h_{p,small} = k_s M^a U_0^b \quad M \leq 1 Kg \quad (24)$$

$$h_{p,large} = k_L \frac{M}{A_p} \log(1 + 5 \times 10^{-5} U_0^2) \quad M > 1 Kg \quad (25)$$

where k_s and k_L are constants for small and large debris respectively. The formula for estimating h_p does not take into consideration the characteristic of the concerned process machinery, as seen in Figures 24 and 25. The parameters for Equations 24 and 25 are mentioned in Table 9.

Table 9.

In Lee's textbook, constant values for particle penetration are given. (Lees, 2004)

Target material	k_s	k_L	a	b
Concrete	1.8×10^{-5}	1×10^{-3}	0.4	1.5
Steel	6.0×10^{-5}	5×10^{-5}	0.3	1
Brickwork	2.3×10^{-5}	2.5×10^{-3}	0.4	1.5

Nguyen et al. (2009) suggested a more reliable formula for calculating a projectile's penetration depth h_p (m). Equations 26 and 27 in the model take into account both the qualities of the effect material and the characteristics of the target material.

Penetration depth (case $\alpha \neq 0$):

$$h_p = \frac{\left(-d_p \cos(\alpha) + \sqrt{\left(d_p \cos(\alpha) \right)^2 + \frac{4}{\pi} \tan(\alpha) \left(\frac{E_c}{f_u \varepsilon_u} \right)^{\frac{2}{3}}} \right)}{2 \tan(\alpha)} \quad (26)$$

Penetration depth (case $\alpha = 0$):

$$h_p = \left(\frac{E_c}{f_u * \varepsilon_u} \right)^{\frac{2}{3}} * \frac{1}{\pi * d_p} \quad (27)$$

where the kinetic energy is defined as $E_c = \frac{M * U_0^2}{2}$ ($Kg * m^2 / s^2$),

f_u and ε_u are the ultimate strength and ultimate strain of the targets constitutive material (Pa), respectively. The penetrating scheme of a rod projectile is seen in Figure 34, where $e_t=t$ is the target thickness and $l_p=h$ is the fragment length.

Since the object and structures dragged by the wind have odd geometries, instead of considering actual fragments, the projectiles are thought to be circular or rod-shaped. In the case of projectile rods, the corresponding diameter must be calculated as a function of their length l_p and area A_p .

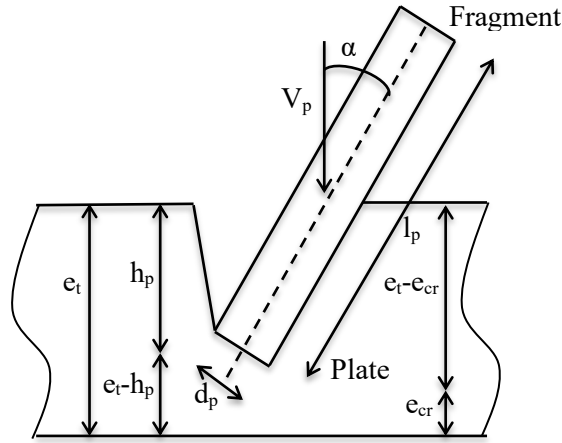


Figure 34. A projectile's (fragment's) impact on a target (a plate) (Nguyen et al., 2009)

The following expression is used to measure the corresponding diameter:

$$d_p = \frac{\left(\sqrt{(\pi * l_p)^2 + 2 * \pi * A_D} - \pi * l_p \right)}{\pi} \quad (28)$$

In addition, the impact force will be compared to the tank's resistance force F_r (N), which is expressed by the equation:

$$F_r = P_r A_p \quad (29)$$

Where P_r is the tank's resistance pressure as determined by Equation 8, and A_p is the object area (m²).

The API-620 specification specifies minimum thicknesses based on the diameter of the tank. The critical thickness (e_{cr}) for the shell of the storage tank would be considered to be this value (Table 10)

$$Damage = \begin{cases} \text{if } F_{ob} - F_r > 0 & \text{Damage} \\ \text{if } F_{ob} - F_r \leq 0 & \text{No damage} \end{cases} \quad (30)$$

Table 10.

Plate thickness requirements for various diameters (American Petroleum Institute, 2013)

Tank diameter (m)	Minimum thicknesses (mm)
≤ 15.2	4.8
$> 7.6 - 18.3$	6.4
$> 18.3 - 30.5$	8
> 30.5	9.6

Equations 22 and 29 will be used to evaluate whether the tank is at risk of being damaged by debris impact drag caused by the storm. The damage parameters for debris effect are presented in Equation 30.

3.2 Wind load effects (local standard TN and Q 2.01.07-85)

To calculate the impact of wind load on industrial equipment in Azerbaijan, reference is made to the following normative documents:

TN and Q 2.01.07-85*	Loads and effects
TN and Q 2.02.01-83*	Ground foundations of buildings and structures
TN and Q 2.03.01-84	Concrete and reinforced concrete structures

3.2.1 Structures parameters and Wind loads

It is important to consider the following wind loads for buildings and structures.

- a) the main type of wind loads;
- b) peak values of wind loads affecting the protective structural elements and their connecting elements;
- c) resonant eddy effects;
- d) variable aerodynamically unstable oscillations of the sprinting, divergence and flatter types.

Resonant vortex effects of wind effects and variable aerodynamic instability oscillations of the rush type $h/d > 10$ (where h is the height, d is the width characteristic of the storage tank) should be taken into account in the relevant buildings and solid-walled structures.

3.2.2 Calculation of wind load

The normative value of wind load w must be given by one of two options. In the first case, the load w is determined by the following aggregates:

- a) normal pressures applied to the outer surface of the device or elements - w_e ;
- b) the friction force w_f directed at touching the outer surface and applied to its horizontal (for beam roofs, partly for glass staircase or corrugated roofs) or vertical projection area (for loggia walls as well as structures).
- c) conductive protection for wind in openings or openings permanently open, normal pressure w_i applied to the inner surface of wall installations;

In the second case, the load w is treated as the sum of the following:

- a) external loads, w_x and w_y projections directed along the x and y axes, conditioned by the total resistance of the devices;
- b) torque with respect to the z axis, w_z .

The normative value of wind loads w is the average w_m and pulsation, which are its components w_p should be defined as the sum of the values:

$$w = w_m + w_p \quad (31)$$

It is allowed not to take into account the pulsation composition of the wind load in determining the internal pressures w_i .

The average normative values of wind load w_m , depending on the equivalent z_e height above the ground, should be determined as follows:

$$w_m = w_0 k(z_e) c \quad (32)$$

where:

w_0 - normative value of wind pressure;

$k(z_e)$ – coefficient taking into account changes in wind pressure at altitude z_e ;

c - aerodynamic coefficient;

Normative values of wind pressure w_0 are accepted according to Table ## depending on windy regions. Normative values of wind pressure are determined on the basis of indicators of meteorological stations of the Hydrometeorological Service of the Republic of Azerbaijan in accordance with the established procedure. In this case, the normative value of wind pressure w_0 is determined in pascals (Pa).

$$w = 0,43 V^2, \text{ (Pa)} \quad (33)$$

Table 11.

Wind regions (according to Map 3)	Ia*	I*	II*	III*	IV*	V	VI	VII*
w_0 , kPa	0,17	0,23	0,30	0,38	0,48	0,60	0,73	0,85
<p><i>Note.</i> * Based on the zoning of the territories of the Republic of Azerbaijan according to the level of normative values of wind pressure, these regions are excluded from the territory of the Republic of Azerbaijan and are included in these norms in terms of feasibility of our national norms in design practice in other countries.</p>								

The equivalent height is determined as follows:

1. For devices such as tower installations, dor, pipe, etc.: $z_e = z$
2. For the following structures:
 - a) When $h \leq d \rightarrow z_e = h$
 - b) When $h \leq 2d$
for $z \geq h - d \rightarrow z_e = h$
for $0 < z < h - d \rightarrow z_e = d$
 - c) When $h > 2d$ for $z \geq h - d \rightarrow z_e = h$; f o r $d < z < h - d \rightarrow z_e = z$;

where:

z – height from the ground;

d – dimensions of the building in the direction perpendicular to the calculated wind direction (width, transverse dimension) (excluding the foundation for columns);

h – the height of the structure.

The coefficient $k(z_e)$ is determined according to Table 12 and formula (34). In this case, the following types of areas are accepted:

- A - open shores of seas, lakes and reservoirs, rural areas, including additional buildings less than 10 m in height, deserts, steppes, forest steppes;
- B - urban areas, forests and other areas regularly covered with obstacles higher than 10 m;
- C - densely built urban areas with buildings higher than 25 m.

$$k(z_e) = k_{10} (z_e/10)^{2a} \quad (43)$$

Table 12

Height z_e , m	Coefficient $k(z_e)$ for given area		
	A	B	C
≤ 5	0,75	0,5	0,4
10	1,0	0,65	0,4
20	1,25	0,85	0,55
40	1,5	1,1	0,8
60	1,7	1,3	1,0
80	1,85	1,45	1,15
100	2,0	1,6	1,25
150	2,25	1,9	1,55
200	2,45	2,1	1,8
250	2,65	2,3	2,0
300	2,75	2,5	2,2
350	2,75	2,75	2,35
≥ 480	2,75	2,75	2,75

The values of k_{10} and α parameters for different types of areas are given in Table 13.

Table 13

Parameter	Area		
	A	B	C
α	0,15	0,20	0,25
K_{10}	1,0	0,65	0,4
ζ_{10}	0,76	1,06	1,78

Table 14

Height z_e , m	Pulsation coefficient ζ of wind pressure for a given area type		
	A	B	C
≤ 5	0,85	1,22	1,78
10	0,76	1,06	1,78
20	0,69	0,92	1,50
40	0,62	0,80	1,26
60	0,58	0,74	1,14
80	0,56	0,70	1,06
100	0,54	0,67	1,00
150	0,51	0,62	0,90
200	0,49	0,58	0,84
250	0,47	0,56	0,80
300	0,46	0,54	0,76
350	0,46	0,52	0,73
≥ 480	0,46	0,50	0,68

3.2.3 Peak wind load

Normative values of the effects of peak wind loads for protective elements and their fastening nodes are determined by the following formula: positive w_+ and negative w_- :

$$w_{+(-)} = w_0 k(z_e) [1 + \zeta(z_e)] c_{p,+(-)} v_{+(-)} \quad (44)$$

where:

w_0 - is the calculated value of wind pressures;

z_e - equivalent height;

$k(z_e)$ and $\zeta(z_e)$ - are the coefficients that take into account the change and beating of wind pressures at the height of z_e .

$c_{p,+(-)}$ - positive pressure (+) and (-) are the maximum values of the absorption aerodynamic coefficients; $v_{+(-)}$ - is the correlation coefficient corresponding to the positive pressure (+) or absorption (-) of the wind load; The values of these coefficients are given in Table 15, depending on the area A of the protective structures where the wind load is collected.

Table 15

A, m^2	<2	5	10	>20
v_+	1,0	0,9	0,8	0,75
v_-	1,0	0,85	0,75	0,65

a) The coefficient C_x for different parts of the structure is determined as follows.

b) $z_e = h$.

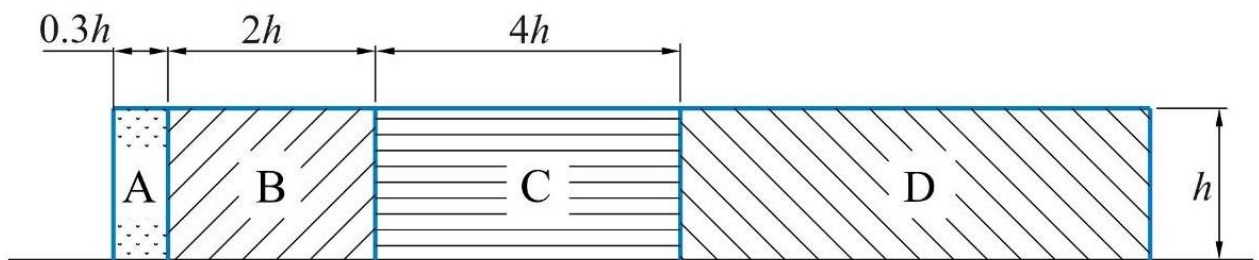


Figure 35.

Table 16

Solid structural parts with a flat surface on the ground			
A	B	C	D
2,1	1,8	1,4	1,2

Rectangular double-sided covered buildings

The vertical wall of the building is rectangular in plan

Table 17

Side walls			Wind effected wall	Wind no-effect wall
Areas				
A	B	C	D	E
-1,0	-0,8	-0,5	0,8	-0,5

Aerodynamic coefficients are given in Table 17. For different areas of the side walls that are wind effected, wind no effected and different.

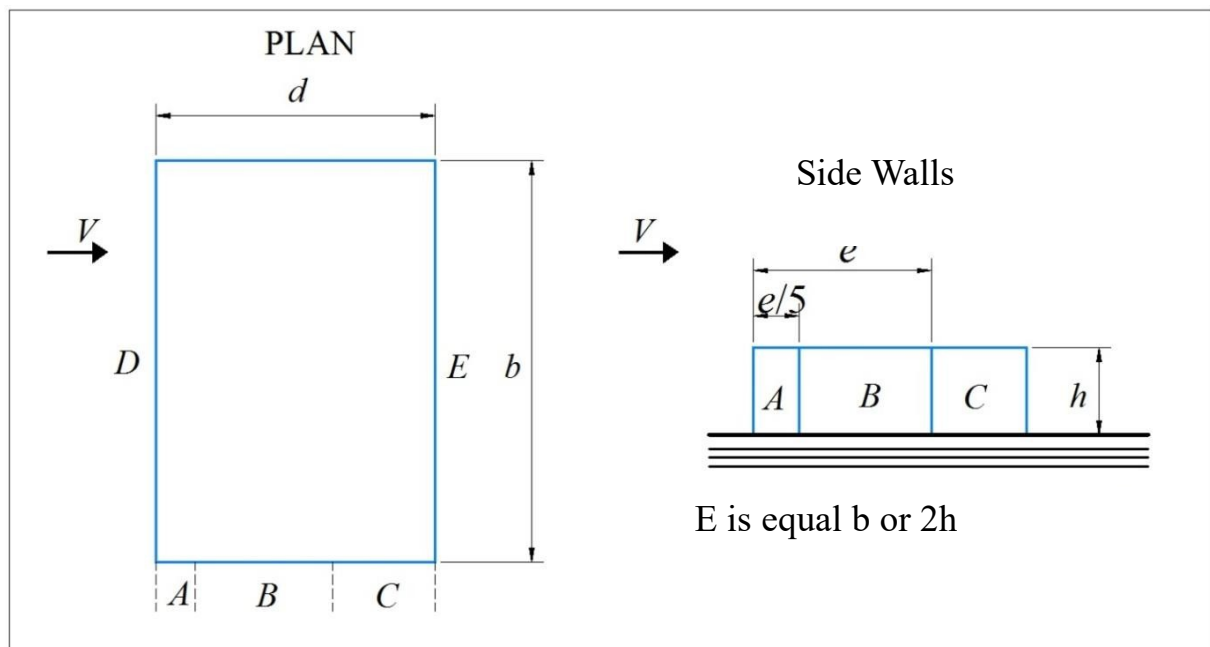


Figure 36.

Double-sided roofing

- For different areas of the cover (Figure 37), the coefficient c_e is determined according to Tables 18 and 19 depending on the direction of the average wind speed;
- For angles $15^\circ \leq \beta \leq 30^\circ$ when $\alpha = 0^\circ$, the calculation of the calculated wind load should be considered in two variants;
- For smooth coatings of a certain size, the aerodynamic coefficient of friction is $c_f = 0.02$ when $\alpha = 90^\circ$.

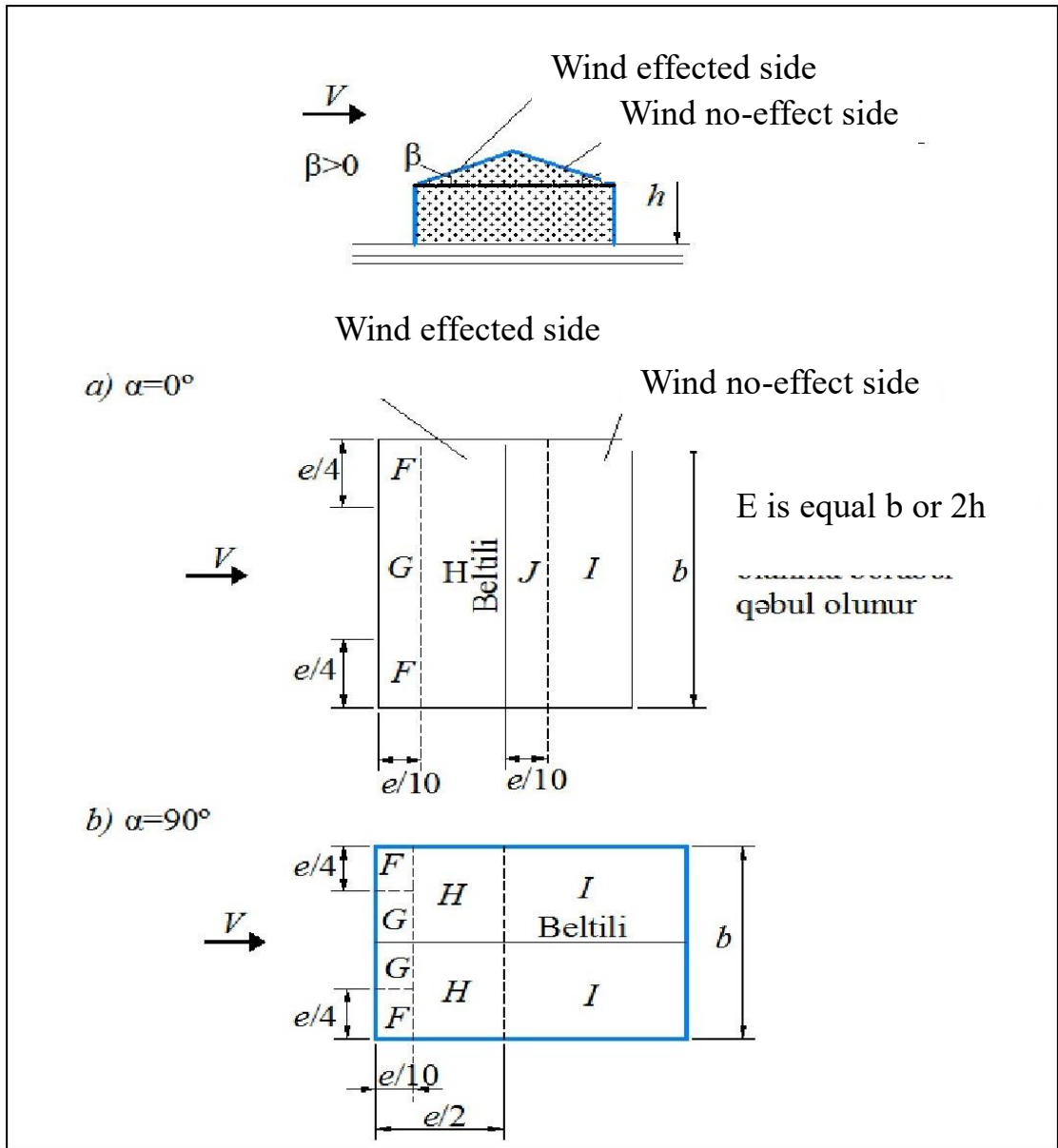


Figure 37.

Table 18

($\alpha = 0^\circ$)

Inclination β	F	G	H	I	J
15°	-0,9	-0,8	-0,3	-0,4	-1,0
	0,2	0,2	0,2		
30°	-0,5	-0,5	-0,2	-0,4	-0,5
	0,7	0,7	0,4		
45°	0,7	0,7	0,6	-0,2	-0,3
60°	0,7	0,7	0,7	-0,2	-0,3
75°	0,8	0,8	0,8	-0,2	-0,3

Table 19
 $(\alpha = 90^\circ)$

β	F	G	H	I
0°	-1,8	-1,3	-0,7	-0,5
15°	-1,3	-1,3	-0,6	-0,5
30°	-1,1	-1,4	-0,8	-0,5
45°	-1,1	-1,4	-0,9	-0,5
60°	-1,1	-1,2	-0,8	-0,5
75°	-1,1	-1,2	-0,8	-0,5

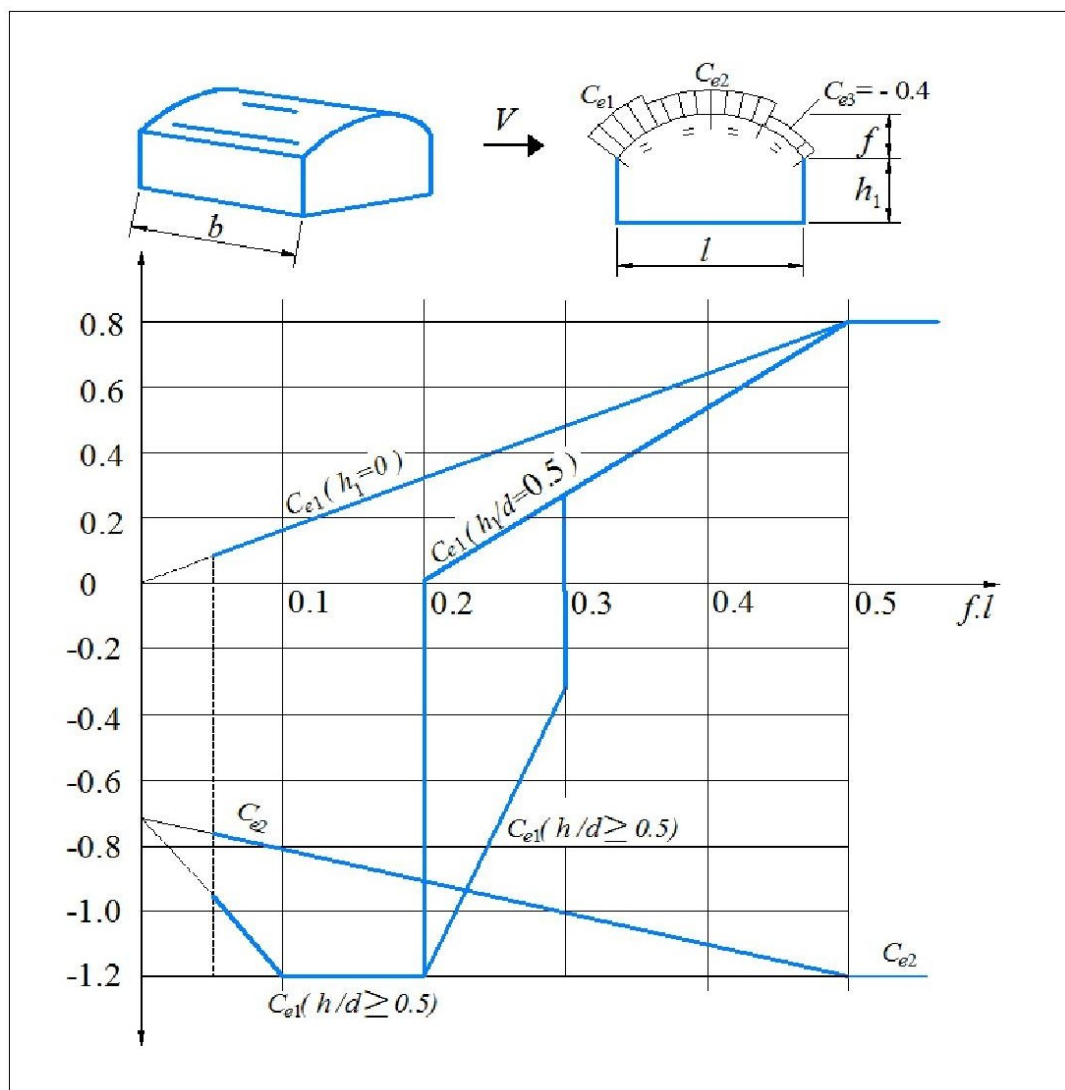


Figure 38. Rectangular buildings with arched and adjacent roofs

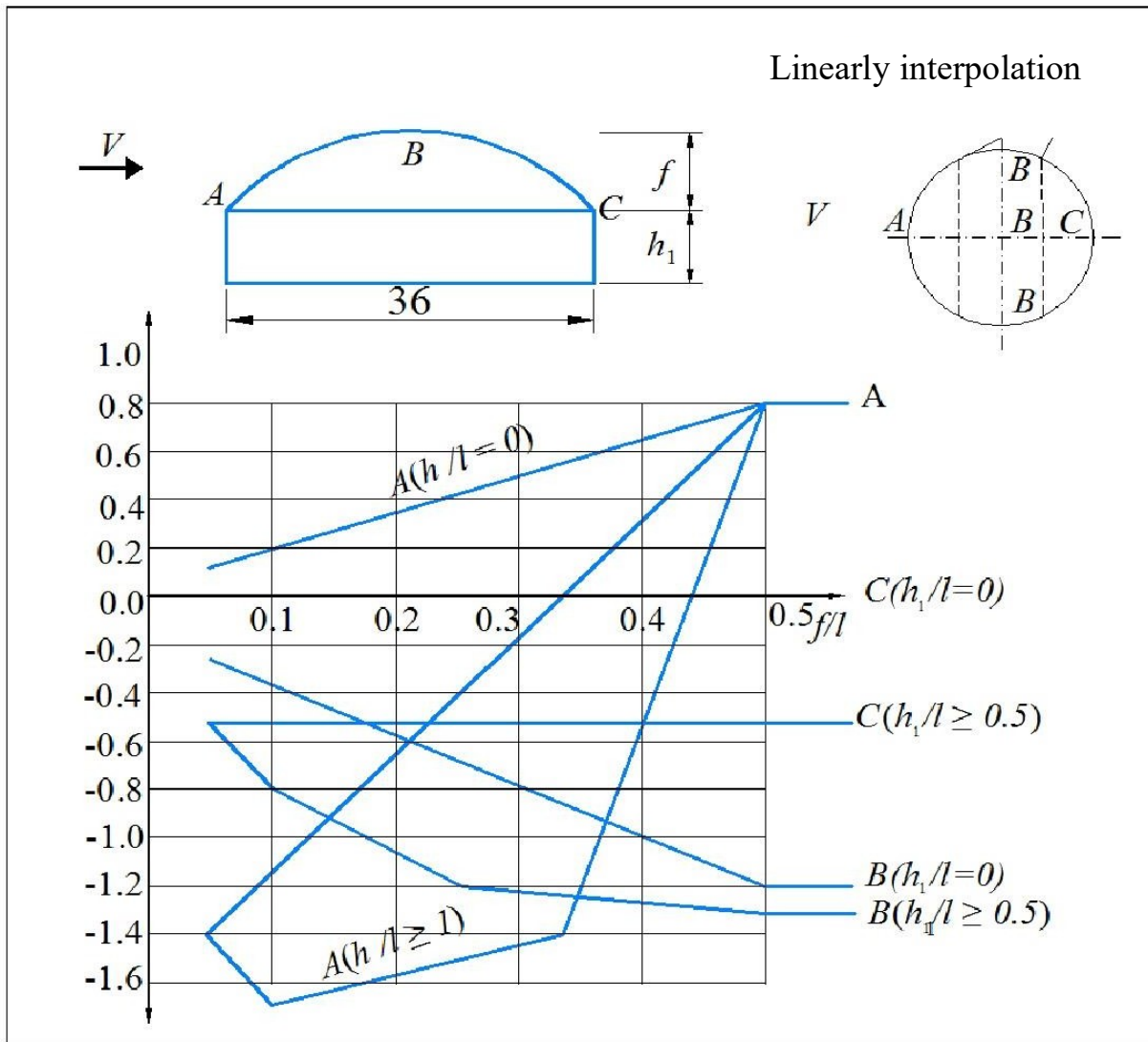


Figure 39. Round buildings with domed roof

Sphere

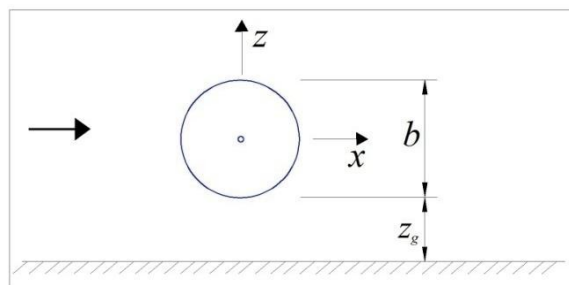


Figure 40.

- a) When $z_g > d/2$ (Figure 40), the aerodynamic coefficients c_x of the front resistances of the spheres depending on the Reynolds Re number and the relative roughness $\delta = \Delta/d$ are given in Figure 41. Here: Δ (m) is the roughness of the surface. If $z_g > d/2$, the value of the coefficient c_x must be

increased 1.6 times.

b) The lifting force coefficient of the sphere c_z is accepted based on the following:

a. when $z_g > b/2 - c_z = 0$;

b. when $z_g < b/2 - c_z = 0.6$.

c) Equivalent height:

$$z_e = z_g + d/2;$$

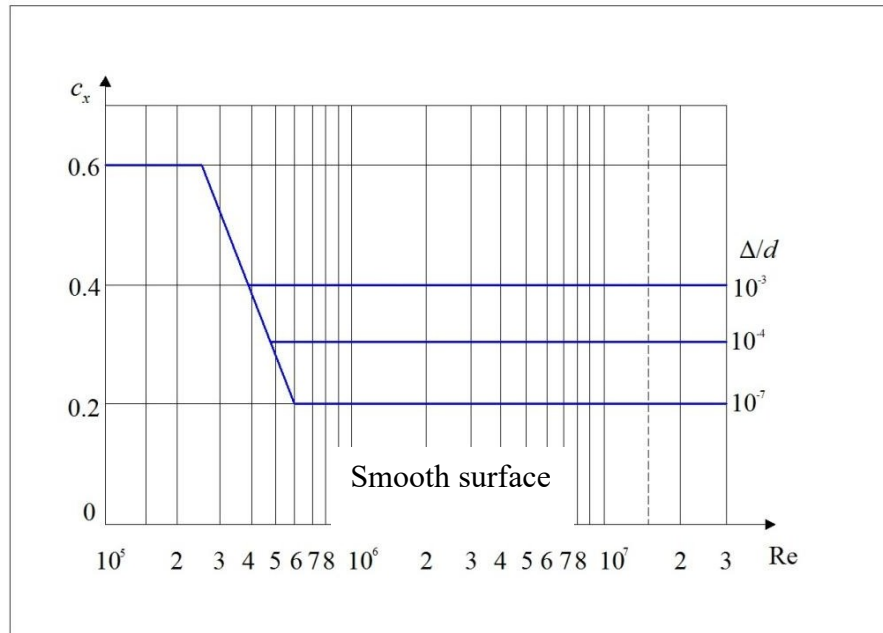


Figure 41.

3.2.4 Calculation of wind load effect on storage tanks

As located offshore, most of tanks are affected by strong winds. In Azerbaijan, during the year, most of time strong winds are seen locally. For estimating the wind load, besides API 650/620, local standard (TN and Q 2.01.07-85) is also used as mentioned above. To compare the results obtained from both standard, real numbers using in the field in Azerbaijan is used in this chapter.

Wind force related to the standard is calculating with the Equation 45:

$$F = C_f \cdot q \cdot A_e \quad 45$$

where:

q - dynamic wind pressure [N/m^2], and estimating like following:

$$q = k \cdot V^2 \quad 46$$

where:

k - constant, in this case is equal to 0,613;

V - basic wind speed;

Ae - effective area [mm²] calculating as follow:

$$A_e = h \cdot D_{ef} \quad 47$$

where:

h - height of element;

D_{ef} – effective diameter, and calculating as follow:

$$D_{ef} = (D_i + 2 \cdot t + 2 \cdot t_{ins}) \quad 48$$

where:

D_i - internal diameter;

t - vessel thickness;

t_{ins} - insulation thickness;

4. Results and discussions

Bearing in mind the materials and methods previously explained, in this chapter are presented some results concerning different aspects as the wind effect on storage tanks obtained employing different methods. Each of them is analyzed in detail and compared. For the sake of clarity, a division into sub-chapters was applied.

4.1 Calculation results of wind effect (API 620 and API 650)

In this section, all the results deriving from the experimental acquisition will be analyzed.

As mentioned above, the effect of wind loading on oil tanks manifests itself in 3 forms: shell buckling; overturning and object impact. Calculations were made in all three directions accordingly.

4.1.1 Shell buckling

The Table 20 shows the tank parameters used in the report for shell buckling. Depending on the parameters, calculation carried out related to the cases shown in the Table 21.

Table 20.

Parameters of tanks for shell buckling calculations

Case 1	ρf [kg/m³]	H [m]
	0,85	11,92
	G	Φ
	9,81	0,1
	Pf [MPa]	H [m]
	9,939492	1,192
Case 2	ρf [kg/m³]	H [m]
	0,85	17,88
	G	Φ
	9,81	0,1
	Pf [MPa]	H [m]
	14,909238	1,788

In the report carried out in accordance with the wind speed and oil storage tank parameters, the minimum and maximum wind speed values were set for Azerbaijan accordingly. The strongest ash speed was set at 40.3 m/s. Khazri wind rarely has the highest price range of 35-40 m/s.

As discussed earlier, the storage tank must be either empty or 10-15% full for buckling to occur. The report took 10% of the liquid volume in the tank. Diesel was used as the liquid type. (density - 0.850 kg/m³).

Calculations were made for the tank wall thickness according to the formulas presented in the report, and the final result was compared with real figures. Appropriate compliance was taken into account in the report.

In calculation of P_{cr} and P_r different kinds of shell thickness are taken into consideration. Main parameters of design of storage tanks are considered for local using tanks.

Table 21.

Parameters of tanks for P_{cr} and its result

E [Pa]	t [m]	H [m]	D[m]	n	v	P_{cr} [MPa]
Case 1						
210000	0,003	11,92	4,56	3	0,3	34,54
210000	0,004	11,92	4,56	3	0,3	46,06
210000	0,005	11,92	4,56	3	0,3	57,57
210000	0,006	11,92	4,56	3	0,3	69,09
210000	0,007	11,92	4,56	3	0,3	80,61
210000	0,008	11,92	4,56	3	0,3	92,13
210000	0,009	11,92	4,56	3	0,3	103,65
Case 2						
210000	0,003	17,88	4,56	3	0,3	34,54
210000	0,004	17,88	4,56	3	0,3	46,06
210000	0,005	17,88	4,56	3	0,3	57,57
210000	0,006	17,88	4,56	3	0,3	69,09
210000	0,007	17,88	4,56	3	0,3	80,61
210000	0,008	17,88	4,56	3	0,3	92,13
210000	0,009	17,88	4,56	3	0,3	103,65

As a shell material type steel is used and all related parameters are considered related to the target material. The difference between cases is heights and thicknesses. The result of calculation for P_r is given in the Table 22. Following equation is used to calculate P_r:

$$P_r = P_f + P_{cr}$$

Following step is to calculate velocity pressure. In the chapter 2, two equations were mentioned, however, based on the international system of units following equation is used in calculation:

$$q_z = 0.613K_zK_{zt}K_dV^2IG_s \left[\frac{N}{m^2} = Pa \right]$$

Table 22.

Parameters of tanks for Pr and its result

Pr [MPa]	
Case 1	Case 2
44,48	49,45
55,99	60,96
67,51	72,48
79,03	84,00
90,55	95,52
102,07	107,04
113,59	118,56

Velocity pressure varies based on the part of the shell. In this reason, it has been calculated for shell roof and shell body separately and given in the Table 23.

Table 23.

Velocity pressure calculation results based on the shell body and shell roof.

for shell	body	for shell	roof
Kz	0,902	Kz	1,073
Kzt	1	Kzt	1
Kd	0,95	Kd	0,85
V	20	V	40
I	1	I	1
Gs	0,85	Gs	0,9
qz	178,595098	qz	805,084776
p	121,444667	p	579,661039
Cp	0,8	Cp	0,8
Pw	121,444667	Pw	579,661039
		Uw	724,576298

To analyze the results last parameter needed is uniform external pressure shown in the Figure 41. For calculating the parameter, following equations were used and results are given in the Table 24:

$$q_{eq} = k_w p_{max}$$

$$k_w = 0.46 \left(1 + 0.1 \sqrt{\frac{(C_{\theta} r)}{(\omega t)}} \right)$$

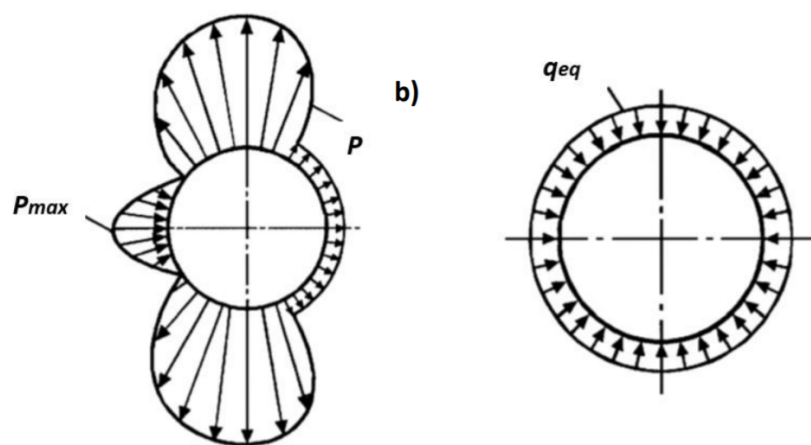


Figure 41.

Table 24.

Parameters of tanks for q_{eq} and its result

C(teta)	R [m]	omega	t [m]	k_w	q_{eq} [Mpa]
0,5	2,28	24,1	0,003	0,642659014	78,05
0,5	2,28	24,1	0,004	0,618187346	75,08
0,5	2,28	24,1	0,005	0,601487064	73,05
0,5	2,28	24,1	0,006	0,589159427	71,55
0,5	2,28	24,1	0,007	0,579578394	70,39
0,5	2,28	24,1	0,008	0,571855345	69,45
0,5	2,28	24,1	0,009	0,565458231	68,67

The equilibrium between the wind loads acting on the tank and the tank's resistance pressure determines whether the machinery will be affected by buckling or discoloration of its shell as the tank is exposed to strong winds. Results are analyzed by taking into account following case characteristics:

$$Damage = \begin{cases} \text{if } q_{eq} - P_r > 0 & \text{Buckling} \\ \text{if } q_{eq} - P_r \leq 0 & \text{No buckling} \end{cases}$$

Results for each case are given in the Table 25.

Table 25.
Results for shell buckling calculation

Case 1			Case 2		
Pr [MPa]	qeq [MPa]	Result	Pr [MPa]	qeq [MPa]	Result
44,48	78,05	Buckling	49,45	78,05	Buckling
55,99	75,08	Buckling	60,96	75,08	Buckling
67,51	73,05	Buckling	72,48	73,05	Buckling
79,03	71,55	No buckling	84,00	71,55	No buckling
90,55	70,39	No buckling	95,52	70,39	No buckling
102,07	69,45	No buckling	107,04	69,45	No buckling
113,59	68,67	No buckling	118,56	68,67	No buckling

4.1.2 Overturning

This chapter discusses the consequences of overturning for storage tanks that are not secured to the ground. The API-650 specification sets standards for non-anchored tanks' stability.

The Table 26 shows the tank parameters used in the report for overturning. Depending on the parameters, calculation carried out related to the cases shown in the Table 26.

Table 26.
Parameters of tanks for overturning calculations

H [m]	D [m]	Ar [m²]	Hr [m]	Pi [MPa]
11,92	4,56	16,32	14	0,124
Dls	Dlr	t [m]	Fby	
17753,3	3496,19	0,006	262	

Below-mentioned equations represents the stability requirement for a non-anchored tank overturning due to an outward wind load:

$$0.6M_w + M_{pi} < \frac{M_{DL}}{1.5} + M_{DLR} \rightarrow F_{o1} < F_{r1}$$

$$M_w + F_p(M_{pi}) < \frac{(M_{DL} + M_F)}{2} + M_{DLR} \rightarrow F_{o2} < F_{r2}$$

For each case following parameters calculations results are shown in the Table 27:

Table 27.

Parameters of tanks parts

For shell		For roof	
Uw		Uw	724,576298
Pw	303,611667	Pw	362,288149

Results obtained the equations are illustrated in the Table 28.

Table 28.

Results of calculatuon of parameters

Mw	Mws	Mpi	Mds
144331,89	167738,966	665,1	40477,524
Mdr	wl	Mf	
7971,3132	12,7344584	415,728517	

By establishing a relationship between the overturning forces F_{oi} produced by the wind on the tank at the time of being impacted by excessive winds and the resistance force of the tank F_{ri} , equations will be used to determine if the equipment will be damaged by overturning.

$$Damage = \begin{cases} \text{if } F_{o1} - F_{r1} > 0 \text{ and } F_{o2} - F_{r2} > 0 & \text{Overturn} \\ \text{If } F_{o1} - F_{r1} \leq 0 \text{ or } F_{o2} - F_{r2} \leq 0 & \text{No overturn} \end{cases}$$

Table 29.

Results for overturning calculation

F01	Fr1	Result
87264,2377	34956,3292	Overturn
F02	Fr2	
144597,931	28417,9395	

4.1.3 Impact of the object

Extreme winds can cause objects to be dragged as they pass. The credibility of a storage tank is jeopardized by these items. When an object is dragged by the storm, it has enough force to kill the components of a storage tank. The force of impact of an object moved by the wind is measured using a combination of forces on the debris that varies depending on the debris properties and wind conditions.

Johnson's number is used in impact dynamics to determine the magnitude of an impact on a continuum that has been filled impetuously and impinged by a preliminary velocity pulse, and it can be determined using the equation below. And results were compared with the Table 30.

$$J' = \frac{U_0^2 M}{\sigma_D t r_p^2}$$

Table 30.

Damage threshold values for Johnson's damage number J' (Salzano & Basco, 2015)

J	Regime	Probability of damage
1x10 ⁻³	Quasi-static elastic	0
1x10 ⁻²	Moderate plastic behavior	0.1
1x10 ⁺¹	Extensive plastic deformation	0.5

The Table 29 shows the tank parameters used in the report for object impact. Depending on the parameters, calculation carried out related to the cases shown in the Table 31.

Table 31.

Parameters of tanks for overturning calculations based on the cases

Case 1		Case 2	
Object parameters		Object parameters	
M	5 kq	M	10 kq
r	15 cm	r	25 cm
type	concrete	type	concrete
lp	20;40;60 cm	lp	20;40;60 cm

Table 32.*Results of calculatuon of Johnson's number based on the cases*

Case 1							Case 2						
Uo	M	sigma	t	rp	J'	Probability	Uo	M	sigma	t	rp	J'	Probability
6	5	215	0,006	0,15	0,000620	0	6	10	215	0,006	0,25	0,000447	0
8	5	215	0,006	0,15	0,001102	0	8	10	215	0,006	0,25	0,000794	0
10	5	215	0,006	0,15	0,001723	0	10	10	215	0,006	0,25	0,001240	0
12	5	215	0,006	0,15	0,002481	0	12	10	215	0,006	0,25	0,001786	0
14	5	215	0,006	0,15	0,003376	0	14	10	215	0,006	0,25	0,002431	0
16	5	215	0,006	0,15	0,004410	0	16	10	215	0,006	0,25	0,003175	0
18	5	215	0,006	0,15	0,005581	0	18	10	215	0,006	0,25	0,004019	0
20	5	215	0,006	0,15	0,006891	0	20	10	215	0,006	0,25	0,004961	0
22	5	215	0,006	0,15	0,008338	0	22	10	215	0,006	0,25	0,006003	0
24	5	215	0,006	0,15	0,009922	0	24	10	215	0,006	0,25	0,007144	0
26	5	215	0,006	0,15	0,011645	0,1	26	10	215	0,006	0,25	0,008384	0
28	5	215	0,006	0,15	0,013506	0,1	28	10	215	0,006	0,25	0,009724	0
30	5	215	0,006	0,15	0,015504	0,1	30	10	215	0,006	0,25	0,011163	0,1
32	5	215	0,006	0,15	0,017640	0,1	32	10	215	0,006	0,25	0,012701	0,1

Following equation was used to determine whether an object will buckle or penetrated a storage tank and results are shown in the Table 33.

$$F_{ob} = \frac{1}{2} \rho_w U_0^2 A_p C_F$$

Table 33.*Results of calculatuon of F_{ob} based on the cases*

ρ_w	A_p	C_f	F_{ob}
Case 1			
1,323	0,07065	0,5	0,84122955
3,136	0,07065	0,5	3,5449344
6,125	0,07065	0,5	10,8182813
10,584	0,07065	0,5	26,9193456
16,807	0,07065	0,5	58,183313
25,088	0,07065	0,5	113,437901
35,721	0,07065	0,5	204,418781
49	0,07065	0,5	346,185
Case 2			
1,323	0,19625	0,5	2,33674875
3,136	0,19625	0,5	9,84704
6,125	0,19625	0,5	30,0507813

10,584	0,19625	0,5	74,77596
16,807	0,19625	0,5	161,620314
25,088	0,19625	0,5	315,10528
35,721	0,19625	0,5	567,829946
49	0,19625	0,5	961,625

Finally, after the tank has been damaged by debris, determining an object's penetration depth h_p (m) from its impact parameters is a practical and practical way to validate Johnson's damage figure. In the case of industrial collisions, the penetration depth of a fragment or debris is a crucial criterion for deciding whether or not industrial machinery has lost its containment.

Table 34.

Parameters of tanks for overturning calculations based on the cases

Ks	Kl	a	b
0,000018	0,001	0,4	1,5
Ec	fu [Mpa]	3u [Mpa]	
90	420	350	

Instead of considering individual fragments, the projectiles are considered to be circular or rod-shaped since the debris and structures dragged by the wind have unusual geometries. The corresponding diameter of projectile rods must be measured as a function of their length l_p and area A_p . To calculate the corresponding diameter, use the following formula and results as given in the Table 35:

$$d_p = \frac{\left(\sqrt{(\pi * l_p)^2 + 2 * \pi * A_D} - \pi * l_p \right)}{\pi}$$

Table 35.

Results of calculatuon of penetration depth based on the cases

dp	alpha	lp	hp	hp (alpha=0)	hp,small	hp,large
Case 1				Case 1		
0,0005624960	10	20	0,00039206	4,08	0,00050363	5,53E-05
0,0005624960	30	20	0,00049245	4,08	0,00077535	9,82E-05
0,0005624960	45	20	0,00080091	4,08	0,00108358	0,000153
0,0005624960	60	20	0,00088235	4,08	0,00142434	0,000221
0,0005624960	90	20	0,00093341	4,08	0,00179495	0,0003
Case 2					0,00219301	0,000391
0,000562496	10	40	0,00056250	4,08	0,00261679	0,000494
0,000562496	30	40	0,00056250	4,08	0,00306482	0,000609
0,000562496	45	40	0,00056250	4,08	Case 2	

0,000562496	60	40	0,00156247	4,08	0,00066451	3,98E-05
0,001562469	90	40	0,00156247	4,08	0,00102308	7,07E-05
Case 3					0,00142979	0,00011
0,00037500	10	60	0,001041658	6,12337079	0,00187951	0,000159
0,00037500	30	60	0,001041658	6,12337079	0,00236845	0,000216
0,00037500	45	60	0,001041658	6,12337079	0,00289369	0,000281
0,00037500	60	60	0,001041658	6,12337079	0,00345288	0,000356
0,00104166	90	60	0,001041658	6,12337079	0,00404406	0,000438

Following equations shows the damage cases for the object effect and results are given in the Table 36:

$$Damage = \begin{cases} \text{if } F_{ob} - F_r > 0 & \text{Damage} \\ \text{if } F_{ob} - F_r \leq 0 & \text{No damage} \end{cases}$$

Table 36

Pr	Fr	Result	Pr	Fr	Result
Case 1			Case 2		
34,54	4,8805805	No damage	34,54	13,557168	No damage
46,06	6,50759918	No damage	46,06	18,0766643	No damage
57,57	8,13475374	Damage	57,57	22,5965379	Damage
69,09	9,76207814	Damage	69,09	27,1168833	Damage
80,61	11,3896063	Damage	80,61	31,6377947	Damage
92,13	13,0173723	Damage	92,13	36,1593666	Damage
103,65	14,6454101	Damage	103,65	40,6816932	Damage

4.2 Calculation results of wind effect (TN and Q 2.01.07-85)

In Azerbaijan as mentioned above, strong winds are common seen, and the industrial equipment safety are calculated based international, Russian and local standards. Local standard TN and Q 2.01.07-85 is prepared taking into consideration Russian standard (СП 20.13330.2011 СНиП 2.01.07-85). In this chapter, wind loading effect on storage tanks are calculated based on the local standard used in Azerbaijan. In Table 37, the data related to the storage tank is given. All data in this chapter is taken from the Azeri Chirag Guneshli (ACG) field which is most famous field in Azerbaijan.

Table 37*Parameters of storage tank*

ELEMENT	Erection	Operation	F.V.	Shutdown	Hydrotest	Elevation
Nozzle N3	10	10	10	10	10	2675
Water (test)					440	2410
Top head	190	190	190	190	190	2380
Shell	690	690	690	690	690	1100
Nozzle N1	10	10	10	10	10	2100
Nozzle N2	10	10	10	10	10	200
Nozzle N4	10	10	10	10	10	1025
Nozzle H1	125	125	125	125	125	350
Water (test)					3250	1100
Fluid (operation)		1625				550
Bottom head	190	190	190	190	190	-180
Fluid (operation)		440				-210
Water (test)					440	-210
Nozzle N5	10	10	10	10	10	-480
Skirt	275	275	275	275	275	-466
TOTAL WEIGHT	1520	3585	1520	1520	5650	kg
				from B.T.L.	from grade	
Elevations for calculation:	Bottom tangent line			0	915	mm
		Base ring		-875	40	mm

4.2.1 Calculation of wind loading

Firstly, for calculation effective diameter of the tank is required and is estimated with the Equation and results are given in the Table 38.

Table 38.*Results of calculation of the effective diameter*

Effective diameters:	Def [cm]			
	Di	t	tins	Def
Top head	1400	0,9	0	1400,18
Shell	1400	0,9	0	1400,18
Bott. head	1400	0,9	0	1400,18
Skirt	1400	0,9	0	1400,18

In this chapter, while the real design data of storage tank is available, and based on this, test calculation are carried out by parameters mentioned in the Table 39.

Table 39.

Results of calculation of wind shear force

DESIGN			[N/m ²]	Aef = Def·	h [cm ²]	[N]	
	H top	H bottom	q	h	Def	F	
Top head	2350	1950	1097	400	1400,18	622	
Shell	1950	50	1097	1900	1400,18	2955	
Bott. head	50	-57	1097	107	1400,18	166	
Skirt	-57	-875	1097	818	1400,18	1272	
TOTAL WIND SHEAR FORCE						5016	N
TEST			[N/m ²]	Aef = Def·	h [mm ²]	[N]	
	H top	H bottom	q	h	Def	F	
Top head	2350	1950	274	400	1400,18	156	
Shell	1950	50	274	1900	1400,18	739	
Bott. head	50	-57	274	107	1400,18	42	
Skirt	-57	-875	274	818	1400,18	318	
TOTAL WIND SHEAR FORCE						1254	N

The next is calculation of the dynamic wind pressure. As given in the design, for test, the calculation is done, and results are given in the Table 40.

Table 40.

Results of calculation of dynamic wind pressure

Design		
k	V	q
0,613	42,3	1096,83477

Test		
k	V	q
0,613	6	22,068
0,613	8	39,232
0,613	10	61,3

0,613	12	88,272
0,613	14	120,148
0,613	16	156,928
0,613	18	198,612
0,613	20	245,2
0,613	22	296,692
0,613	24	353,088
0,613	26	414,388
0,613	28	480,592
0,613	30	551,7
0,613	32	627,712
0,613	34	708,628
0,613	36	794,448
0,613	38	885,172
0,613	40	980,8
0,613	42	1081,332
0,613	44	1186,768

Ae - effective area [cm²] is calculated by using following equation and results are shown in the Table 41.

$$A_e = h \cdot D_{ef}$$

47

Table 41.

Results of calculation of affective area

Design							
part	Di	t	Def	Htop	Hbottom	dh	Ae
top head	1400	0,009	1400,018	2350	1950	400	560007,2
shell	1400	0,009	1400,018	1950	50	1900	2660034,2
bottom head	1400	0,009	1400,018	50	-57	107	149801,926

skirt	1400	0,009	1400,018	-57	-875	818	1145214,72
-------	------	-------	----------	-----	------	-----	------------

Test							
part	Di	t	Def	Htop	Hbottom	dh	Ae
top head	1400	0,009	1400,018	2350	1950	400	560007,2
shell	1400	0,009	1400,018	1950	50	1900	2660034,2
bottom head	1400	0,009	1400,018	50	-57	107	149801,926
skirt	1400	0,009	1400,018	-57	-875	818	1145214,72

Shear forces and bending moments at different levels is calculated and the results are given in the Table 42:

Table 42

Results of calculation of Shear forces and bending moments at different level

Elevation -57			Level 858			
Shear [N]			Distance		Moment [N·mm]	
Design	Test			Design	Test	
622	156		2207	1373029	343257	
2955	739		1057	3123532	780883	
166	42		54	8903	2226	
3744	936	N	TOTAL	4505465	1126366 N·mm	
Elevation -875			Level 40			
Shear [N]			Distance		Moment [N·mm]	
Design	Test			Design	Test	
				4505465	1126366	
3744	936		818	3062294	765573	
1272	318		409	520348	130087	
5016	1254	N	TOTAL	8088107	2022027 N·mm	

TOTAL WIND LOADING AT CALCULATION ELEVATIONS:

An increment factor of 1,6 is included in wind load to Take into account piping. Refer to "Pressure Vessel Design Manual" (D.R. Moss), Table 3-4.

Table 43.

Results of calculation of Shear forces and bending moments at different level

Elevation -57	Level 858					
	Erection	Operation	F.V.	Shutdown	Test	
SHEAR:	5990	5990	5990	5990	1497	N
MOMENT:	7208744	7208744	7208744	7208744	1802186	N·mm

Elevation -875	Level 40					
	Erection	Operation	F.V.	Shutdown	Test	
SHEAR:	8025	8025	8025	8025	2006	N
MOMENT:	12940971	12940971	12940971	12940971	3235243	N·mm

The stability of the storage tank is tested based on the given design data and following results are obtained and shown in the Table 44:

Table 44.

Results of calculation of the stability of the storage tank

Design		
part	Cf	F
top head	1	305
shell	1	1448
bottom head	1	82

Test											
part	Cf	F, V=6	F, V=8	F, V=10	F, V=12	F, V=14	F, V=16	F, V=18	F, V=20	F, V=22	F, V=24
top head	1	12	22	34	49	67	88	111	137	166	198
shell	1	59	104	163	235	320	417	528	652	789	939
bottom head	1	3	6	9	13	18	24	30	37	44	53
skirt	1	25	45	70	101	138	180	227	281	340	404
part	Cf	F, V=26	F, V=28	F, V=30	F, V=32	F, V=34	F, V=36	F, V=38	F, V=40	F, V=42	F, V=44
top head	1	232	269	309	352	397	445	496	549	606	665
shell	1	1102	1278	1468	1670	1885	2113	2355	2609	2876	3157
bottom head	1	62	72	83	94	106	119	133	147	162	178
skirt	1	475	550	632	719	812	910	1014	1123	1238	1359

As we can see, when the wind speed is exceeded the which was considered during the design phase, and also as the tank usage period is increasing, the destabilization occurs, and it can be easily seen in the Table 44.

4.3 Comparison of the results

In this final chapter, the obtained results will be compared and discussed.

First of all, a comparison between the results obtained from API 620 and API 650 and TN and Q 2.01.07-85 is discussed. To do that, some parity figures and tables comparing the two approaches are presented. In addition to that, some graphs reporting Pf and Pcr are reported. As explained before, in this case, only the parameters of local used storage tanks were considered.

Starting from the analysis of the results obtained from the equations, some aspects can be noted: 1) for the storage tanks using in Azerbaijan, some parameters are only considered during local standard calculations. However, for application of the equations provided by API 620/API650 classified tables are used as a reference. 2) In report, especially for local calculations, field data received from Azeri Chirag Gunashli (one of the main oil fields in Azerbaijan) is used and following calculations proceeded. 3) In the process of calculation based on API standards, three types of wind effect were taking into consideration, while implementing the local calculation only direct wind loading effect were considered.

The second aspect concerns the distance between the results found based on the similar tank parameters. The latter varies depending on the considered effective height, in particular, it is rather low if we consider the diameter of the tank and increases with the increase of the fluid included itself. As explained before, for what concern 10 % of the fluid, just a single point has been taken into account for the effective height calculation because as explained before buckling effect is only available when the percent is lower than 15%.

The third is about the overturning of the tank. As seen in the previous chapters, both with the equational model and with the experimental data for overturning of the storage tank based on the overturning moment is noted. In this case, for locally used storage tanks given data and wind speed considered in the report shows that overturning effect can occur. This is explained by the fact that if this was not the case, clearly there would not have an increasing trend of the damage between the data displayed in the tables, and test is just done for showing the possibility. In real report, design characteristics take into account the frequency of probability of seeing the strong wind in Azerbaijan, mainly in Baku where most of the storage tanks are locating.

Shell buckling results are given by the parameters namely: the resistance pressures, the uniform external pressure. Case of the possibility of shell buckling damage is given by the following equations:

$$Damage = \begin{cases} \text{if } q_{eq} - P_r > 0 & \text{Buckling} \\ \text{if } q_{eq} - P_r \leq 0 & \text{No buckling} \end{cases}$$

From the table, it can be seen that for by increasing the wing speed, the possibility of buckling effects is also increased as well.

Case 1			Case 2		
Pr [MPa]	qeq [MPa]	Result	Pr [MPa]	qeq [MPa]	Result
44,48	78,05	Buckling	49,45	78,05	Buckling
55,99	75,08	Buckling	60,96	75,08	Buckling
67,51	73,05	Buckling	72,48	73,05	Buckling
79,03	71,55	No buckling	84,00	71,55	No buckling
90,55	70,39	No buckling	95,52	70,39	No buckling
102,07	69,45	No buckling	107,04	69,45	No buckling
113,59	68,67	No buckling	118,56	68,67	No buckling

Overturning effect results are given by the parameters namely: the overturning forces, the resistance force. Case of the possibility of overturning damage is given by the following equations:

$$Damage = \begin{cases} \text{if } F_{o1} - F_{r1} > 0 \text{ and } F_{o2} - F_{r2} > 0 & \text{Overturn} \\ \text{If } F_{o1} - F_{r1} \leq 0 \text{ or } F_{o2} - F_{r2} \leq 0 & \text{No overturn} \end{cases}$$

From the table, it can be seen that for by increasing the wing speed, the possibility of overturning is also increased as well. Damage scenario is reported because of having an idea about the real situation and design characteristics.

F ₀₁	F _{r1}	Result
87264,2377	34956,3292	Overturn
F ₀₂	F _{r2}	
144597,931	28417,9395	

Results of calculations of object impact are given by the parameters namely: the impact force, the resistance force. For calculation the impact of the object, the material of the object is taken as concrete, and weight is considered as a common object found in the field easily which helped to estimate real situation. Case of the possibility of the damage of the object impact is given by the following equations:

$$Damage = \begin{cases} \text{if } F_{ob} - F_r > 0 & \text{Damage} \\ \text{if } F_{ob} - F_r \leq 0 & \text{No damage} \end{cases} \quad (30)$$

Pr	Fr	Result	Pr	Fr	Result
Case 1			Case 2		
34,54	4,8805805	No damage	34,54	13,557168	No damage
46,06	6,50759918	No damage	46,06	18,0766643	No damage
57,57	8,13475374	Damage	57,57	22,5965379	Damage
69,09	9,76207814	Damage	69,09	27,1168833	Damage
80,61	11,3896063	Damage	80,61	31,6377947	Damage
92,13	13,0173723	Damage	92,13	36,1593666	Damage
103,65	14,6454101	Damage	103,65	40,6816932	Damage

As it has been seen from the table, while increasing the wind speed, the impact of the object is risen up as well. Damage scenario is established for finding the result possibility of the damage occurred by the object. Although taking into account small values for the parameters of the object, the damage situation is also seen. Real wind frequency and gust is also considered. For local calculations, the real design data obtained using local standard is referred. Test results were compared with the design results and results are given in the below-mentioned table.

Test											
part	Cf	F, V=6	F, V=8	F, V=10	F, V=12	F, V=14	F, V=16	F, V=18	F, V=20	F, V=22	F, V=24
top head	1	12	22	34	49	67	88	111	137	166	198
shell	1	59	104	163	235	320	417	528	652	789	939
bottom head	1	3	6	9	13	18	24	30	37	44	53
skirt	1	25	45	70	101	138	180	227	281	340	404
part	Cf	F, V=26	F, V=28	F, V=30	F, V=32	F, V=34	F, V=36	F, V=38	F, V=40	F, V=42	F, V=44
top head	1	232	269	309	352	397	445	496	549	606	665
shell	1	1102	1278	1468	1670	1885	2113	2355	2609	2876	3157
bottom head	1	62	72	83	94	106	119	133	147	162	178
skirt	1	475	550	632	719	812	910	1014	1123	1238	1359

As we can see, when the wind speed is exceeded the which was considered during the design phase, and also as the tank usage period is increasing, the destabilization occurs, and it can be easily seen in the Table. In case of a future project concerning, for example, the building of an oil storage station, the Equational model, based on Equations considered cases, is the most efficient so far. For example, Sangachal oil terminal is the biggest oil storage station in Azerbaijan, and API 620/650 standards were considered besides local standards.

5. Conclusions

This thesis focuses on the unintended consequences that can occur if a vertical storage tank fails during a flood, earthquake, or storm surge that results in high wind loads. The proposed approach is a straightforward, systematic, and repeatable framework for integrating qualitative and quantitative data on the causes and effects of industrial accidents. It enables a researcher to determine the probability of NaTech events triggered by various natural events while taking into account the variability or uncertainty of parameters associated with the natural occurrence.

The results from each of the studied hazards (wind loads, hydraulic loads, and seismic forces) were computed and analyzed in the case study, which aims to reflect the conditions of real infrastructure in Colombia. In terms of the influence of input parameters, such as the fill level of the storage tank, on damage probabilities and the action of fragility curves, the findings were consistent with previous research. Furthermore, the proposed loss methodology was used to calculate the estimated losses due to the tank's structural damages. Subsequently, for the input hazards, this contributes to the computation of threats and potential effects, which is extremely useful for feeding risk reduction systems elsewhere.

The buckling behavior of cylindrical open-topped steel tanks during wind load is investigated in this thesis. For functional tanks, the stability carrying capacity of wind load declines as the aspect ratio falls. As a result, it is anticipated that larger tanks with a lower aspect ratio would be more vulnerable to buckling during a windstorm.

Tanks have a higher buckling resistance under wind load than they do under uniform strain, with a deviation of about 25–50 percent. For a preliminary assessment of the wind buckling critical load, the critical uniform pressure of buckling based on theory may be used. The wind buckling resistance of the tank is greatly reduced when the shell thickness is reduced. Corrosion allowance should be considered in the design of cylindrical shells, and certain measurements should be taken to increase corrosion resistance. The accumulated liquid contributes significantly to the tank's wind buckling resistance.

Wind speed [m/s]	Frequency [%]	Impact type	Standards				Impact type	Standards			
			API 620/650		TN and Q			API 620/650		TN and Q	
			Result		Result			Result		Result	
				Pr.		Pr.			Pr.		Pr.
<6	40,8	Shell buckling	No Buckling	0	No Buckling	0	Overturning	No damage	0	No damage	0
6 - 10	17,4		No Buckling	0	No Buckling	0		No damage	0	No damage	0
10 - 15	12,7		No Buckling	0	No Buckling	0		No damage	0	No damage	0
16 - 20	10,3		No Buckling	0	No Buckling	0		No damage	0	No damage	0
21 - 25	9,1		No Buckling	0	No Buckling	0		No damage	0	No damage	0
26-30	5,6		Buckling	1	Buckling	1		Damage	1	No damage	0
30+	4,1		Buckling	1	Buckling	1		Damage	1	Damage	1

Another form of damage that may occur as a result of an excessive wind load is the overturning of a storage tank. Some scholars believe that this is one of the least likely forms of damage to occur, and that when it does, the storage tank must be empty or partly empty. The API-650 standard (American Petroleum Institute, 2007) does, however, define some stability requirements (overturning stability) that can be used to build a storage tank that is subjected to high wind loads. And it happens when the tank's anchored structure is weak or not fully anchored.

Wind speed [m/s]	Frequency [%]	Impact type	API 620/650		Impact type	API 620/650	
			Result			Result	
				Pr.			Pr.
			<6	40,8		Object Impact (Case 1)	No damage
6 - 10	17,4	No damage	0	No damage	0		
10 - 15	12,7	No damage	0	No damage	0		
16 - 20	10,3	No damage	0	No damage	0		
21 - 25	9,1	No damage	0	Damage	10		
26-30	5,6	Damage	10	Damage	10		
30+	4,1	Damage	10	Damage	10		

The objective of this thesis is to analyze and assess natural hazards (such as hurricanes and tornadoes) and their effect on vertical storage tanks in order to predict the likelihood of a NaTech incident. Since storage tanks may hold large quantities of hazardous material, it's critical to assess the conditions under which a tank may collapse, taking into account various types of damage. Given that this is one of the input parameters to the conventional risk analysis, estimating the harm likelihood due to the effects of a natural hazard is critical.

6. Bibliography

In English

1. Allaby, M. (2007). *Encyclopedia of Weather and Climate*. Facts on File Science Library.
2. American Petroleum Institute. (2013). *API STD 620—Design and Construction of Large, Welded, Low-pressure Storage Tanks*. American Petroleum Institute.
3. Antonioni, G., Landucci, G., Necci, A., Gheorghiu, D., & Cozzani, V. (2015). Quantitative assessment of risk due to NaTech scenarios caused by floods. *Reliability Engineering & System Safety*, *142*, 334–345. <https://doi.org/10.1016/j.res.2015.05.020>
4. Antonioni, G., Spadoni, G., & Cozzani, V. (2007). A methodology for the quantitative risk assessment of major accidents triggered by seismic events. *Journal of Hazardous Materials*, *147*(1), 48–59. <https://doi.org/10.1016/j.jhazmat.2006.12.043>
5. Campedel, M. (2008). *Analysis of Major Industrial Accidents Triggered by Natural Events Reported In the Principal Available Chemical Accident Databases*. European Commission, Joint Research Centre.
6. Cozzani, V., Antonioni, G., Landucci, G., Tugnoli, A., Bonvicini, S., & Spadoni, G. (2014). Quantitative assessment of domino and NaTech scenarios in complex industrial areas. *Journal of Loss Prevention in the Process Industries*, *28*, 10–22. <https://doi.org/10.1016/j.jlp.2013.07.009>
7. El Hajj, C., Piatyszek, E., Tardy, A., & Laforest, V. (2015). Development of generic bow-tie diagrams of accidental scenarios triggered by flooding of industrial facilities (Natech). *Journal of Loss Prevention in the Process Industries*, *36*, 72–83. <https://doi.org/10.1016/j.jlp.2015.05.003>
8. European committee for standardization. (2005). *Eurocode 1: Actions on structures—Part 1-4: General actions—Wind actions*. European committee for standardization.
9. Landucci, G., Antonioni, G., Tugnoli, A., & Cozzani, V. (2012). Release of hazardous substances in flood events: Damage model for atmospheric storage tanks. *Reliability Engineering & System Safety*, *106*, 200–216. <https://doi.org/10.1016/j.res.2012.05.010>
10. Landucci, G., Necci, A., Antonioni, G., Tugnoli, A., & Cozzani, V. (2014). Release of hazardous substances in flood events: Damage model for horizontal cylindrical vessels. *Reliability Engineering & System Safety*, *132*, 125–145. <https://doi.org/10.1016/j.res.2014.07.016>

11. Lees, F. (2004). Lees' Loss Prevention in the Process Industries: Hazard Identification, Assessment and Control: Third Edition. In *Lees' Loss Prevention in the Process Industries: Hazard Identification, Assessment and Control* (3rd ed). Butterworth-Heinemann.
<https://doi.org/10.1016/B978-0-7506-7555-0.X5081-6>
12. Misuri, A., Antonioni, G., & Cozzani, V. (2020). Quantitative risk assessment of domino effect in Natech scenarios triggered by lightning. *Journal of Loss Prevention in the Process Industries*, 64, 104095. <https://doi.org/10.1016/j.jlp.2020.104095>
13. Munich RE. (2019). *Natural disaster risks: Losses are trending upwards*. Risks Posed by Natural Disasters. <https://www.munichre.com/en/risks/natural-disasters-losses-are-trending-upwards.html#1995343501>
14. Necci, A., Antonioni, G., Bonvicini, S., & Cozzani, V. (2016). Quantitative assessment of risk due to major accidents triggered by lightning. *Reliability Engineering & System Safety*, 154, 60–72. <https://doi.org/10.1016/j.ress.2016.05.009>
15. Nguyen, Q. B., Mebarki, A., Saada, R. A., Mercier, F., & Reimeringer, M. (2009). Integrated probabilistic framework for domino effect and risk analysis. *Advances in Engineering Software*, 40(9), 892–901. <https://doi.org/10.1016/j.advengsoft.2009.01.002>
16. Ocampo, F. (2016). Marco para el tratamiento de incertidumbre en el análisis de riesgo cuantitativo en transporte de material peligroso a través de tuberías. In *Departamento de Ingeniería Química: Vol. Master's*. Universidad de los Andes.
17. Potter, T. D., & Colman, B. R. (2003). *Handbook of Weather, Climate, and Water: Dynamics, Climate, Physical Meteorology, Weather Systems, and Measurements*. Wiley-Interscience.
18. Ramírez Olivar, O. J., Mayorga, S. Z., Giraldo, F. M., Sánchez-Silva, M., Pinelli, J.-P., & Salzano, E. (2020). The effects of extreme winds on atmospheric storage tanks. *Reliability Engineering & System Safety*, 195, 106686. <https://doi.org/10.1016/j.ress.2019.106686>
19. Salzano, E., & Basco, A. (2015). Simplified model for the evaluation of the effects of explosions on industrial target. *Journal of Loss Prevention in the Process Industries*, 37, 119–123. <https://doi.org/10.1016/j.jlp.2015.07.005>
20. Salzano, E., Iervolino, I., & Fabbrocino, G. (2003). Seismic risk of atmospheric storage tanks in the framework of quantitative risk analysis. *Journal of Loss Prevention in the Process Industries*, 16(5), 403–409. [https://doi.org/10.1016/S0950-4230\(03\)00052-4](https://doi.org/10.1016/S0950-4230(03)00052-4)
21. Villalba, N. (2016). *Marco de referencia para el análisis del riesgo asociado a eventos Natech provocados por inundaciones*. Universidad de los Andes.

In Azerbaijani

1. A.Məsimov. *ABƏŞ və ARDNŞ-in Xəzər dənizinin Azərbaycan Respublikası sektorunda birgə fəaliyyətinin yekunlarına dair [Mətn]*
2. Tex. üzrə fəls. d-ru e. dər. al. üçün təq. ed. dis.: 05.11.01 /U. Q. Məmmədov; *Magistral boru kəmərlərinin rezervuar parklarında nəql olunan neftin əsas parametrlərini ölçən qurğular [Mətn]*: Azərb. Dövlət Neft Akademiyası. Bakı: 2011.
3. *Neft emalı zavodları rezervuar və nasoslarının istismarında təhlükəsizlik texnikası [Mətn] : əmtəə operatorları üçün mühazirələr konspekti* /Neft Sənayesi Nazirliyi, Ümumittifaq Elmi-Tədqiqat Təhlükəsizlik Texnikası İn-tu ; [tərt. ed. E. E. Qlaz ; red. K. S. Mehdiyev]. Bakı: Azərneftnəşr, 1952.
4. H. R. Qurbanov, F. Q. Seyfiyev, Ə. N. Qurbanov, E. X. İskəndərov ; elmi red. Q. Q. İsmayılov. *Neftin, qazın saxlanması qurğularının istismarı [Mətn]: dərs vəsaiti* / Azərb. Dövlət Neft və Sənaye Un-ti. Bakı: [s. n.], 2016.
5. T. Sadıqov. *Rezervuarlar və boru kəmərləri [Mətn]*.
6. *Yüklər və Təsirlər Layihələndirmə Normaları*. Azərbaycan Respublikası Dövlət Şəhərsalma və Arxitektura Komitəsinin Kollegiyasının 15 aprel 2015-ci il tarixli 02№-li qərarı ilə təsdiq edilmişdir.

In Russian

1. Ч. С. Агаларов; [ред. М. Д. Оруджев ; худож. В. Цейтин. *Вопросы комплексной автоматизации резервуарных парков и нефтебаз [Текст]*.
2. Б. Т. Бадагуев. *Работы с повышенной опасностью. Работы в колодцах, каналах, отстойниках, резервуарах [Текст] : [практическое пособие]*
3. А. М. Архаров, И. Д. Кунис; Под ред. И. В. Бармина. *Криогенные заправочные системы стартовых ракетно-космических комплексов [Текст]*
4. М. К. Сафарян Москва: Недра, 1987. *Металлические резервуары и газгольдеры [Текст]*.
5. М. И. Ашкинази Москва: Гостоптехиздат, 1960. *Резервуары со сфероцилиндрической крышей [Электронный ресурс] : опыт строительства и эксплуатации*
6. А. В. Кирюхин, И. Ф. Делемень, Д. Н. Гусев; Москва: Наука, 1991. *Высокотемпературные гидротермальные резервуары [Текст]*. отв. ред. В. М. Сугробов; АН СССР, Дальневосточное Отделение Ордена Трудового Красного Знамени Ин-тут Вулканологии.